NASA TECHNICAL NOTE

NASA TN D-7754

NASA TN D-7754

AN ANALYTICAL STUDY OF THE EFFECTS OF JETS LOCATED MORE THAN ONE JET DIAMETER ABOVE A WING AT SUBSONIC SPEEDS

by Lawrence E. Putnam

Langley Research Center
Hampton, Va. 23665

NATIONAL AERONAUTICS AND SPACE ADMINISTRATION • WASHINGTON, D. C. • AUGUST 1974

1. Report No.	2. Government Accession No.	3. Recipient's Catalog No.
NASA TN D-7754		

4. Title and Subtitle	5. Report Date
AN ANALYTICAL STUDY OF THE EFFECTS OF JETS LOCATED MORE THAN ONE JET DIAMETER ABOVE A WING AT SUBSONIC SPEEDS	August 1974
	6. Performing Organization Code

7. Author(s)	8. Performing Organization Report No.
Lawrence E. Putnam	L-9683
	10. Work Unit No. 501-24-06-01

9. Performing Organization Name and Address	11. Contract or Grant No.
NASA Langley Research Center Hampton, Va. 23665	
	13. Type of Report and Period Covered
12. Sponsoring Agency Name and Address	Technical Note
National Aeronautics and Space Administration Washington, D.C. 20546	14. Sponsoring Agency Code

15. Supplementary Notes

16. Abstract

A procedure has been developed for calculating the effects of blowing two jets over a swept tapered wing at low subsonic speeds. The algorithm used is based on a vortex-lattice representation of the wing lifting surface and a line sink-source distribution to simulate the effects of the jet exhaust on the wing lift and drag. The method is limited to those cases in which the jet exhaust does not intersect or wash the wing. The predictions of this relatively simple procedure are in remarkably good agreement with experimentally measured interference lift and interference induced drag.

17. Key Words (Suggested by Author(s))	18. Distribution Statement
Aerodynamics Subsonic flow Upper surface blowing Jet interaction	Unclassified – Unlimited STAR Category 01

19. Security Classif. (of this report)	20. Security Classif. (of this page)	21. No. of Pages	22. Price*
Unclassified	Unclassified	41	$3.25

*For sale by the National Technical Information Service, Springfield, Virginia 22151

AN ANALYTICAL STUDY OF THE EFFECTS OF JETS LOCATED MORE THAN ONE JET DIAMETER ABOVE A WING AT SUBSONIC SPEEDS

By Lawrence E. Putnam
Langley Research Center

SUMMARY

A procedure has been developed for calculating the effects of blowing two jets over a swept tapered wing at low subsonic speeds. The algorithm used is based on a vortex-lattice representation of the wing lifting surface and a line sink-source distribution to simulate the effects of the jet exhaust on the wing lift and drag. The method is limited to those cases in which the jet exhaust does not intersect or wash the wing. The predictions of this relatively simple procedure are in remarkably good agreement with experimentally measured interference lift and interference induced drag.

The results of the analytical study have indicated that substantial increases in wing lift and reductions in wing induced drag can occur when jets are blown over a wing. The magnitude of these effects increases with an increasing ratio of jet-exit velocity to free-stream velocity. The results also indicate that the interference effects are the most favorable when the nozzle exits are located ahead of or at the wing leading edge and inboard near the wing center line. The present method does not correctly predict the effects of the vertical location of the jets at jet center-line heights of less than approximately 1.5 jet-exit diameters; however, as the jet vertical location is reduced to this height, the favorable effects of blowing jets over a wing increase.

INTRODUCTION

Recently, there has been renewed interest in locating the propulsion systems of future jet transport airplanes forward and above the wing. This unconventional engine location can take two forms. In one form, the jet is exhausted so that it attaches to the upper surface of the wing to take advantage of Coanda turning of the jet exhaust as it passes over the wing-flap system to achieve high lift. (See refs. 1 to 4.) In the second form, the jet exhaust is raised so that the exhaust flow does not attach to the wing in order to avoid the cruise drag penalties associated with the first form. In both cases, the jet noise propagated below the airplane during take-off and landing may be reduced

by the shielding effects of the wing. (See refs. 5 and 6.) To date, however, there is very little experimental information of relevance, except for references 7 to 9. Furthermore, there are only a limited number of theoretical methods (refs. 10 and 11, for example) available for use in assessing the effects of jets located above a wing on the subsonic cruise and climb performance of future jet transport airplanes.

The purpose of the present study was, therefore, to develop an analytical method by which the effects of jets located above a wing on subsonic cruise and climb performance could be investigated. An elementary analytical procedure has been developed to calculate the effects of blowing one or two jets over a swept tapered wing. This method is based on the vortex-lattice theory for the wing and on the theory of reference 12 for a jet exhausting into a subsonic stream. As a result of the basic assumptions, the method is limited to the case in which the jet exhaust does not intersect or wash the wing. As long as the jet is sufficiently high above the wing so that it does not violate this condition, the effects of the following on the lift and drag induced by blowing jets over a wing at subsonic speeds can be analytically investigated: ratio of jet to free-stream velocity, location of the jet exhaust relative to the wing, nozzle-exit diameter, wing leading-edge sweep, wing aspect ratio, and wing taper ratio.

SYMBOLS

A_e exit area per nozzle

b wing span

C_A axial-force coefficient

$C_{D,i}$ induced-drag coefficient

$\Delta C_{D,i} = (C_{D,i})_{\text{jet on}} - (C_{D,i})_{\text{jet off}}$

C_L lift coefficient

$\Delta C_L = (C_L)_{\text{jet on}} - (C_L)_{\text{jet off}}$

C_N normal-force coefficient

c wing chord or chord of elemental vortex-lattice panel

c_{av} average wing chord, S_{ref}/b

c_e wing chord at η_e

c_l section lift coefficient

d_e nozzle-exit diameter

K_I slope of line-source or line-sink distribution of interval I

l_c length of chordwise vortex-line segment on wing

l_{core} length of core of jet exhaust plume

M Mach number

N number of points or number of elemental vortex-lattice panels

p static pressure

p_t stagnation pressure

Q strength of line-source or line-sink distribution

q dynamic pressure

S_{ref} reference area (wing planform area as shown in fig. 1)

s semiwidth of horseshoe vortex

U longitudinal velocity

u_i, v_i, w_i circulation-induced perturbation-velocity components in positive X-, Y-, and Z-directions

$u_{jet}, v_{jet}, w_{jet}$ jet-induced perturbation-velocity components in positive X-, Y-, and Z-directions

V_e effective velocity ratio, $\sqrt{\frac{\rho_\infty U_\infty^2}{\rho_e U_e^2}}$

V_r	radial velocity in jet axis system induced by line sink-source distribution
X,Y,Z	orthogonal right-handed primary Cartesian coordinate system with origin at wing apex (see fig. 1). Positive X-direction is forward, positive Y-direction is toward right wing tip, and positive Z-direction is downward. XY-plane parallel to wing chord plane
X_{jet},R_{jet}	jet cylindrical coordinate system with origin at nozzle exit (fig. 3); positive X-direction is in direction of jet exhaust
x,r	cylindrical coordinates associated with jet (fig. 3), where a subscript indicates a specific value of each coordinate
$x_{c/4}$	longitudinal location in primary Cartesian coordinate system of midspan point of quarter-chord line of elemental panel (fig. 2)
$x_{3c/4}$	longitudinal location in primary Cartesian coordinate system of midspan point of three-quarter-chord line of elemental panel (fig. 2)
x_e,y_e,z_e	primary Cartesian coordinates of nozzle exit (fig. 1)
x_{le}	primary Cartesian X-coordinate of wing leading edge at y_e (fig. 1)
y_{cp}	primary Cartesian Y-coordinate of control point on elemental panel (fig. 2)
α	angle of attack, degrees
Γ	circulation strength
γ	ratio of specific heats
ζ	dummy variable of integration
η	fraction of wing semispan from wing-root chord in Y-direction
θ	camber angle of wing at control point, degrees
Λ	sweep angle of quarter-chord line of elemental vortex-lattice panel (fig. 2), degrees

$\Lambda_{c/4}$ sweep angle of wing quarter-chord line, degrees

Λ_{le} wing leading-edge sweep angle

λ taper ratio, c_t/c_r

ρ density

Subscripts:

c chordwise

e exit

r root

s spanwise

t tip

total total

∞ free stream

METHOD OF ANALYSIS

The algorithm used in the present study to calculate the effects of exhaust jets located above a swept tapered wing is based on a vortex-lattice representation of the wing lifting surface and a line source-sink distribution to represent the entrainment and blockage effects of the exhaust jets. The method, which has been programed for a digital computer, assumes that the flow is steady, irrotational, and incompressible and that the flow external to the jet exhaust is inviscid. It is also assumed that the jet is not deflected, that the cross-sectional shape of the jet is not distorted by the wing flow field or by the free-stream angle of attack, and that the jets do not interact or wash the wings. No effects of the wing flow field on the entrainment of the jet were considered. Shown in figure 1 is a typical wing planform and engine arrangement for which the effects of blowing jets over the wing can be calculated by the present method. The present computer program does not allow discontinuous wing leading or trailing edges, but these

planforms are not excluded from the present method. Note also that the effects of the nacelles on the wing are neglected with the present method.

The vortex-lattice method used to represent the wing lifting surface is based on references 13 and 14. For the present simplified planforms, each half of the wing is subdivided in both the spanwise and chordwise directions into 50 or less elemental areas. In the present computer program the number of spanwise and chordwise panels is arbitrary; however, unless otherwise specified, all calculations for the present study were made with 5 equally spaced chordwise and 10 equally spaced spanwise divisions on each half of the wing. Each elemental area is represented by a horseshoe vortex with the bound portion lying along the local quarter-chord line of the element. (See fig. 2.) The trailing vortices lie streamwise along the inboard and outboard edges of each panel on the wing-chord plane. Aft of the wing trailing edge, the trailing vortices continue in the chordwise direction; that is, it is assumed that the trailing vortices are not turned by the wing downwash or by the free-stream velocity. Note that this is not the conventional method of locating the trailing vortices parallel to the free-stream velocity, as used in reference 14, but is similar to the formulation of reference 13. The boundary condition that the flow be tangential to the wing surface is satisfied for each element at a control point on the lateral midpoint of the local three-quarter-chord line of the element.

The induced effects of the jet exhaust were simulated with a distribution of line sinks and sources located on the longitudinal axis of the jet. The axis of the jet was divided into a number of segments over which the sink or source strength was assumed to be linear. This continuous line sink-source distribution is equivalent to a series of triangular elemental distributions as illustrated in figure 3. The radial velocity induced by the jet at a point in the surrounding flow field can therefore be obtained by summing the induced velocities resulting from each triangular elemental line source or sink. The radial velocity is therefore given by

$$V_r(x,r) = \frac{K_1 r}{4\pi}\int_{x_1}^{x_2} \frac{(x_2 - \zeta)d\zeta}{\left[(x - \zeta)^2 + r^2\right]^{3/2}} + \sum_{I=2}^{N-1} \frac{K_I r}{4\pi}\left\{\frac{(x_I - x_{I-1})}{(x_{I+1} - x_I)}\int_{x_I}^{x_{I+1}} \frac{(x_{I+1} - \zeta)d\zeta}{\left[(x - \zeta)^2 + r^2\right]^{3/2}}\right.$$

$$\left. + \int_{x_{I-1}}^{x_I} \frac{(\zeta - x_{I-1})d\zeta}{\left[(x - \zeta)^2 + r^2\right]^{3/2}}\right\} + \frac{K_N r}{4\pi}\int_{x_{N-1}}^{x_N} \frac{(\zeta - x_N)d\zeta}{\left[(x - \zeta)^2 + r^2\right]^{3/2}}$$

The slope K_I $(I = 1,N)$ of the line source or sink of each elemental distribution was adjusted to give the inflow velocity on the boundary of the jet predicted by the method of reference 12. In the present analysis only those interference effects resulting from the

jet radial perturbation velocities are considered; any perturbation velocities induced parallel to the jet axis are neglected. In essence, then, the interference effects of the jet on the wing are attributed to an upwash distribution along the wing lifting surface.

In order for the circulation strength of each elemental horseshoe vortex on the wing to be determined, the following equation for the circulation-induced downwash velocity must be satisfied at each control point on the wing:

$$\frac{w_i}{U_\infty} = \frac{\sin(\alpha + \theta)}{\cos \theta} - \frac{w_{jet}}{U_\infty} - \frac{u_{jet}}{U_\infty} \tan \theta$$

A sketch illustrating this boundary condition at each control point is shown in figure 4. It is apparent from this sketch how the induced effects of the jet modify the boundary-condition equation. Note that in the present formulation, the u_{jet} perturbation velocity arises only when the axis of the jet is not parallel to the wing-chord plane.

After the circulation strengths for the horseshoe vortices are determined, the forces acting on the wing can be determined. From reference 13, the forces acting on each spanwise segment of vortex filament in coefficient form are

$$C_{A,s} = \frac{2\Gamma_s}{U_\infty}\left(\frac{w_i}{U_\infty} + \frac{w_{jet}}{U_\infty} - \sin \alpha\right)\left(\frac{2s}{S_{ref}}\right)$$

and

$$C_{N,s} = \frac{2\Gamma_s}{U_\infty}\left[\left(\frac{v_i}{U_\infty} + \frac{v_{jet}}{U_\infty}\right)\tan \Lambda - \frac{u_i}{U_\infty} - \frac{u_{jet}}{U_\infty} + \cos \alpha\right]\left(\frac{2s}{S_{ref}}\right)$$

For each chordwise segment of vortex filament, the force coefficients are

$$C_{A,c} = 0$$

and

$$C_{N,c} = \frac{2\Gamma_c}{U_\infty}\left(\frac{v_i}{U_\infty} + \frac{v_{jet}}{U_\infty}\right)\frac{l_c}{S_{ref}}$$

where Γ_c is the net circulation strength resulting from the individual circulations of each trailing horseshoe-vortex leg forming that segment. The total normal force $C_{N,total}$ and axial force $C_{A,total}$ acting on the wing are obtained by summing the normal and axial forces acting on all segments. The lift and induced-drag coefficients are then obtained from

$$C_L = C_{N,total} \cos \alpha - C_{A,total} \sin \alpha$$

and

$$C_{D,i} = C_{A,total} \cos \alpha + C_{N,total} \sin \alpha$$

This solution for the induced drag is equivalent to the near-field solution of reference 14. The integration of the wing span load distribution (the far-field method) to obtain the induced drag is not applicable to the present problem because the induced upwash field generated by the jet exhaust violates the assumption inherent in the far-field method. (See refs. 15 and 16.)

DISCUSSION

Comparison of Present Method With Other Theoretical Methods and With Experiment

To verify the vortex-lattice algorithm used to represent the wing in the present method, the computed lift and drag characteristics of an aspect-ratio-8 straight wing without jets have been compared to the predictions of reference 14. (See fig. 5.) The present computer algorithm gives essentially the same results as reference 12 for each of the cases considered: a flat wing, a wing with Clark Y camber distribution, and a twisted wing with no camber. (The twisted wing had a linear distribution of twist which varied from -0.25° at the wing root to 4.75° at the wing tip.) Note that the near-field induced-drag results of reference 14 are compared with the present method.

Experimental investigations of the effects of blowing jets over a wing are very scarce for the case in which the jet is sufficiently high to insure that it does not wash the wing. One source of such data is reference 17, where one jet is centered above a wing. The comparison of the present method with these experimental results, shown in figure 6, indicates very good agreement at vertical locations of the jet exhaust greater than 1.5 nozzle-exit diameters above the wing. In general, the effects of the ratio of jet velocity to free-stream velocity and of the vertical distance of the jet above the wing on the interference lift are well predicted. As the jet approaches the wing, however, the experimental results show a significant increase in interference lift over the predicted values. This discrepancy results, in part, from the interference lift associated with Coanda turning of the jet when the jet washes the upper surface of the wing. The effect of Coanda turning of the jet exhaust is, of course, neglected in the present method.

A comparison of the present method with the experimental data of reference 9 (for two air jets blowing over a wing having a 50° swept leading edge with an aspect ratio of 3 and a taper ratio of 0.3) is shown in figure 7. These experimental data were obtained at

ratios of nozzle-exit total pressure to free-stream static pressure from approximately 1 to 6 and at free-stream Mach numbers of 0.4, 0.6, and 0.7. The theory of reference 10 was derived for an incompressible jet exhausting into an incompressible external stream with no density difference between the two streams. The variable-density case can be related to the incompressible constant-density solution of reference 12 with an effective velocity ratio (ref. 18) as defined in the following equation:

$$V_e = \sqrt{\frac{\rho_\infty U_\infty^2}{\rho_e U_e^2}} = \sqrt{\frac{q_\infty}{q_e}} = \frac{M_\infty}{M_e}\sqrt{\frac{\gamma_\infty p_\infty}{\gamma_e p_{t,e}}}\left[1 + \frac{(\gamma_e - 1)}{2} M_e^2\right]^{\gamma_e/2(\gamma_e - 1)}$$

For an air jet with $\gamma_e = \gamma_\infty = 1.4$,

$$V_e = \frac{M_\infty}{M_e}\frac{(1 + 0.2M_e^2)^{7/4}}{\sqrt{p_{t,e}/p_\infty}}$$

As shown in figures 7(a) and 7(b), the effective velocity ratio reasonably correlates the interference lift and the interference induced drag resulting from blowing two air jets over the wing having a 50° swept leading edge (ref. 9) at Mach numbers from 0.4 to 0.7. The predictions of the present method are in good agreement with the experimental results. These results indicate that the present method can be extended by use of the effective-velocity-ratio concept to the case in which the jet and free stream are compressible and are at different densities. (Note that the exit-momentum coefficient of the jet is inversely proportional to the square of the effective velocity ratio and should provide a similar correlation of the data.)

A further application of the present method using the effective-velocity-ratio concept is shown in figure 7(c) for the 50° swept wing of reference 9. Here the following equations were used to obtain the predicted lift and induced drag:

$$(C_L)_{predicted} = (C_{L,jet\ off})_{measured} + (\Delta C_L)_{predicted}$$

at a given α and

$$(C_{D,i})_{predicted} = \left[(C_{D,i})_{jet\ off}\right]_{measured} + (\Delta C_{D,i})_{predicted}$$

at a given C_L. The predicted lift and drag characteristics using the present method to calculate the effects of the jets with these equations are in good agreement with the experimental results. Of particular interest is the agreement of the predictions of the present

method with the experimentally indicated improvement in induced drag (not necessarily in total drag) due to blowing two jets over the wing.

Effect of Vortex-Lattice Arrangement

Shown in figure 8 is the effect of the number of elemental chordwise panels on the predicted lift and induced drag of an aspect-ratio-8, taper-ratio-0.3 wing having the quarter chord swept 0° with and without two jets blowing over the wing. It is apparent that there is essentially no effect of varying the number of chordwise elemental panels on the predicted lift and induced drag of the wing or on the increments in lift and drag due to jet blowing. Varying the number of spanwise elemental panels does result in a change in the predicted lift and induced drag for the wing with and without jet blowing. (See fig. 9.) It appears, however, that the interference effect due to jet blowing is not a strong function of the number of elemental vortex-lattice panels. Therefore, within the limits of the present computer program, the predicted effects of jet blowing are essentially unaffected by vortex-lattice arrangement. For that reason, 5 chordwise and 10 spanwise elemental panels have been used for all calculations of the present paper.

Effect of Velocity Ratio

The predicted effects of effective velocity ratio on the interference lift and interference induced drag due to jet blowing are shown in figures 6, 7, and 10 for an aspect-ratio-2 straight untapered wing, for an aspect-ratio-3, taper-ratio-0.3 wing with a 50° swept leading edge, and for an aspect-ratio-8, taper-ratio-0.3 wing with a 30° swept quarter chord, respectively. The present method predicts an increase in the interference lift coefficient with increasing jet blowing $\left(\text{that is, increasing } 1/V_e\right)$. This favorable interference effect is essentially unaffected by an angle of attack of up to 10°. (See fig. 10(c).) The present method also predicts a decrease in induced drag with an increasing ratio of jet velocity to free-stream velocity $1/V_e$. This favorable increment in interference-induced drag increases with the lift coefficient. (See fig. 10(c).) In figure 10(b) are shown typical calculations of the effects of effective velocity ratio on the wing span load distribution and on the section lift coefficient. Increased jet blowing results in an increased distortion of the span load distribution. Note that this increased distortion does not imply increased induced drag since the integration of the span load distribution to obtain induced drag is only valid for planar wings without external interference effects. As would be expected, the span load does increase in the vicinity of the jet. Increasing jet blowing also increases the section lift coefficient over the entire wing span.

Effect of Jet Location

The predicted effects of jet location on the interference lift and interference induced drag caused by one or two jets blowing over various wing configurations are shown in figures 6 and 11 to 14. Increasing the vertical distance of the jets above the wing (figs. 6 and 11) causes a decrease in the interference lift and a reduction in the favorable interference induced drag. Moving the nozzle exit ahead of the wing leading edge (fig. 12) causes a small increase in the interference lift and a small increase in the favorable induced-drag increment. Moving the nozzle exit aft of the wing leading edge causes a decrease in the interference lift and a substantial reduction in the favorable induced-drag increment. The calculations shown in figures 13 and 14 indicate that the closer the jets are located to the wing center line the more favorable the interference effects caused by blowing two jets over a wing. This is indeed a fortuitous result, since reference 4 indicates that for a two-engine configuration the engine should be located inboard to minimize the engine-out effect on the rolling moment associated with upper surface blowing configurations during take-off and landing.

CONCLUDING REMARKS

A procedure has been developed for calculating the effects of blowing two jets over a swept tapered wing at low subsonic speeds. The algorithm used is based on a vortex-lattice representation of the wing lifting surface and a line sink-source distribution to simulate the effects of the jet exhaust on the wing lift and drag. The method is limited to those cases in which the jet exhaust does not intersect or wash the wing. The predictions of this relatively simple procedure are in remarkably good agreement with experimentally measured interference lift and interference induced drag.

The results of the analytical study have indicated that substantial increases in wing lift and reductions in wing induced drag can occur when jets are blown over a wing. The magnitude of these effects increases with an increasing ratio of jet-exit velocity to free-stream velocity. The results also indicate that the interference effects are the most favorable when the nozzle exits are located ahead of or at the wing leading edge and inboard near the wing center line. The present method does not correctly predict the effects of the vertical location of the jets at jet center-line heights of less than approximately 1.5 jet-exit diameters; however, as the vertical location of the jets is reduced to this height, the favorable effects of blowing jets over a wing increase.

Langley Research Center,
National Aeronautics and Space Administration,
Hampton, Va., July 21, 1974.

REFERENCES

1. Riebe, John M.; and Davenport, Edwin E.: Exploratory Wind-Tunnel Investigation To Determine the Lift Effects of Blowing Over Flaps From Nacelles Mounted Above the Wing. NACA TN 4298, 1958.

2. Turner, Thomas R.; Davenport, Edwin E.; and Riebe, John M.: Low-Speed Investigation of Blowing From Nacelles Mounted Inboard and on the Upper Surface of an Aspect-Ratio-7.0 35° Swept Wing With Fuselage and Various Tail Arrangements. NASA MEMO 5-1-59L, 1959.

3. Phelps, Arthur E., III: Aerodynamics of the Upper Surface Blown Flap. STOL Technology, NASA SP-320, 1972, pp. 97-110.

4. Phelps, Arthur E., III; and Smith, Charles C., Jr.: Wind-Tunnel Investigation of an Upper Surface Blown Jet-Flap Powered-Lift Configuration. NASA TN D-7399, 1973.

5. Anon.: Aircraft Engine Noise Reduction. NASA SP-311, 1972.

6. Dorsch, Robert G.; and Reshotko, Meyer: EBF Noise Tests With Engine Under-the-Wing and Over-the-Wing Configurations. STOL Technology, NASA SP-320, 1972, pp. 455-473.

7. Kettle, D. J.; Kurn, A. G.; and Bagley, J. A.: Exploratory Tests on a Forward-Mounted Overwing Engine Installation. C.P. No. 1207, Brit. A.R.C., 1972.

8. Wimpress, John K.: Upper Surface Blowing Technology as Applied to the YC-14 Airplane. [Preprint] 730916, Soc. Automot. Eng., Oct. 1973.

9. Putnam, Lawrence E.: Exploratory Investigation at Mach Numbers From 0.40 to 0.95 of the Effects of Jets Blown Over a Wing. NASA TN D-7367, 1973.

10. Shollenberger, C. A.: Analysis of the Interaction of Jets and Airfoils in Two Dimensions. J. Aircraft, vol. 10, no. 5, May 1973, pp. 267-273.

11. Lan, C. Edward: An Analytical Investigation of Wing-Jet Interaction. CRINC-FRL 74-001 (NASA Grant 17-002-107), Univ. of Kansas, Apr. 1974. (Available as NASA CR-138140.)

12. Squire H. B.; and Trouncer, J.: Round Jets in a General Stream. R. & M. No. 1974, Brit. A.R.C., 1944.

13. Fox, Charles H., Jr.: Prediction of Lift and Drag for Slender Sharp-Edge Delta Wings in Ground Proximity. NASA TN D-4891, 1969.

14. Margason, Richard J.; and Lamar, John E.: Vortex-Lattice FORTRAN Program for Estimating Subsonic Aerodynamic Characteristics of Complex Planforms. NASA TN D-6142, 1971.

15. Pope, Alan: Basic Wing and Airfoil Theory. First ed., McGraw-Hill Book Co., Inc., 1951, pp. 200-203.

16. Cone, Clarence D., Jr.: The Theory of Induced Lift and Minimum Induced Drag of Nonplanar Lifting Systems. NASA TR R-139, 1962.

17. Falk, H.: The Influence of the Jet of a Propulsion Unit on Nearby Wings. NACA TM 1104, 1946.

18. Carter, Arthur W.: Effects of Jet-Exhaust Location on the Longitudinal Aerodynamic Characteristics of a Jet V/STOL Model. NASA TN D-5333, 1969.

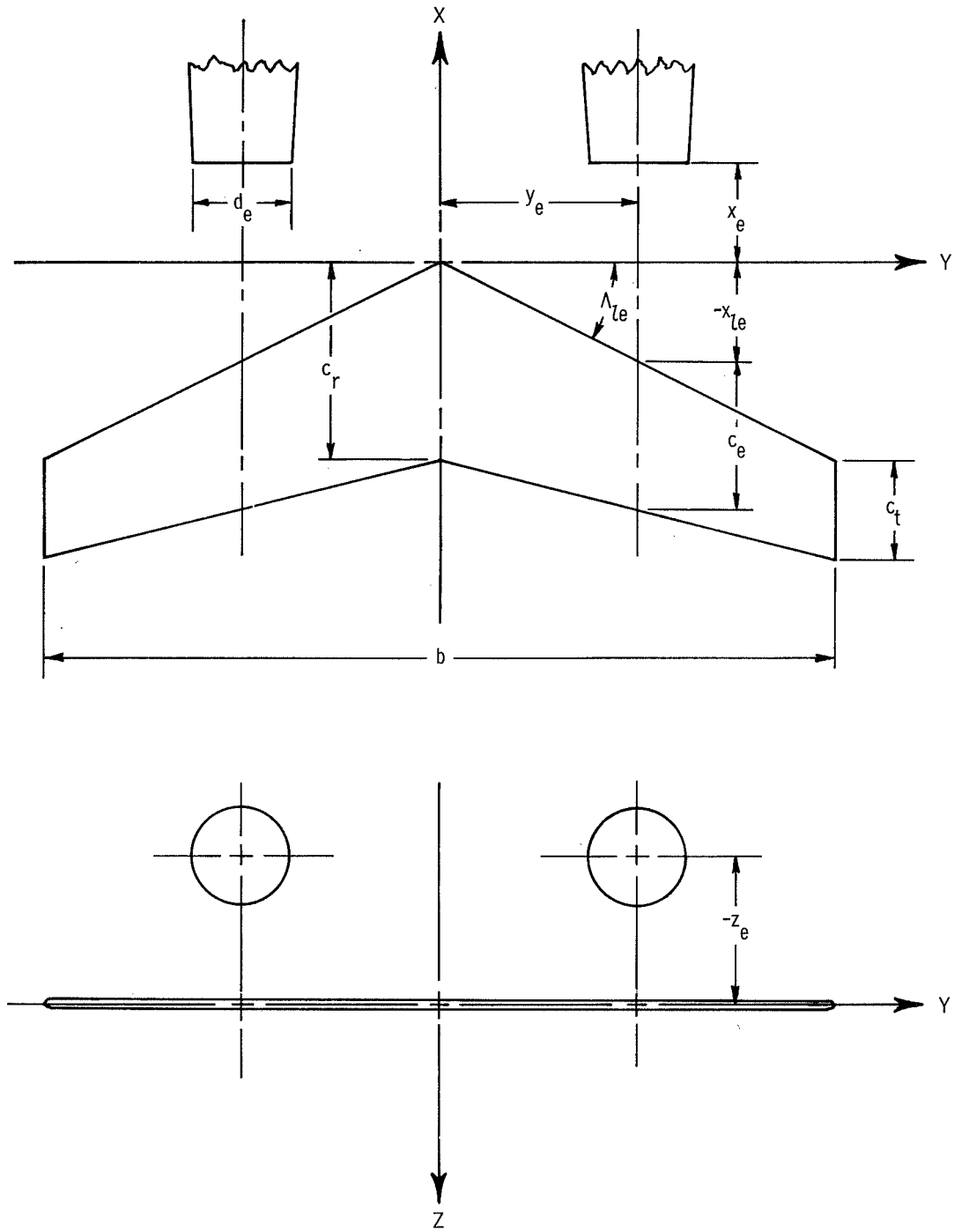

Figure 1.- General layout of a typical wing planform showing axis system and location of nozzle exits.

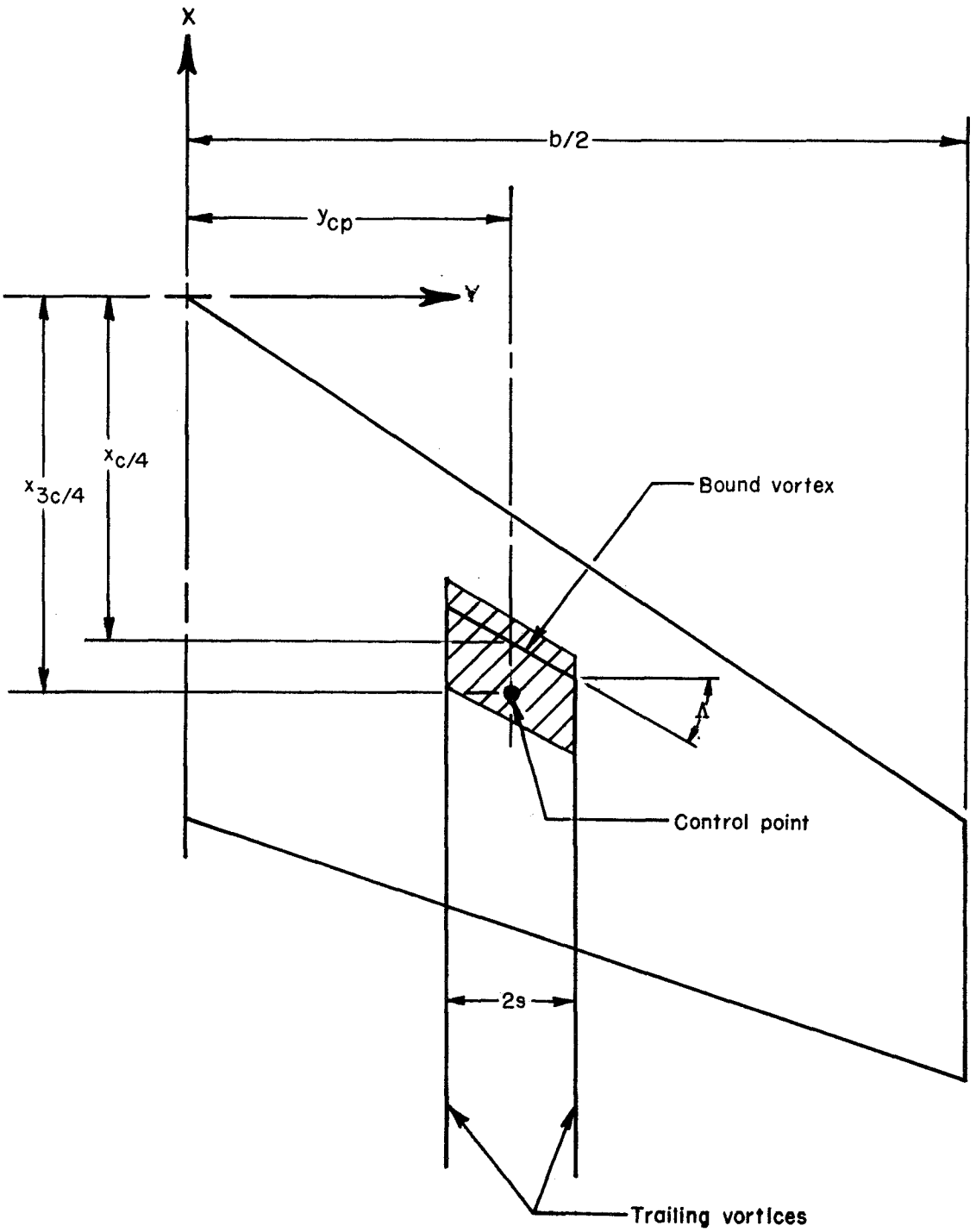

Figure 2.- Sketch of a typical elemental vortex-lattice panel on a wing.

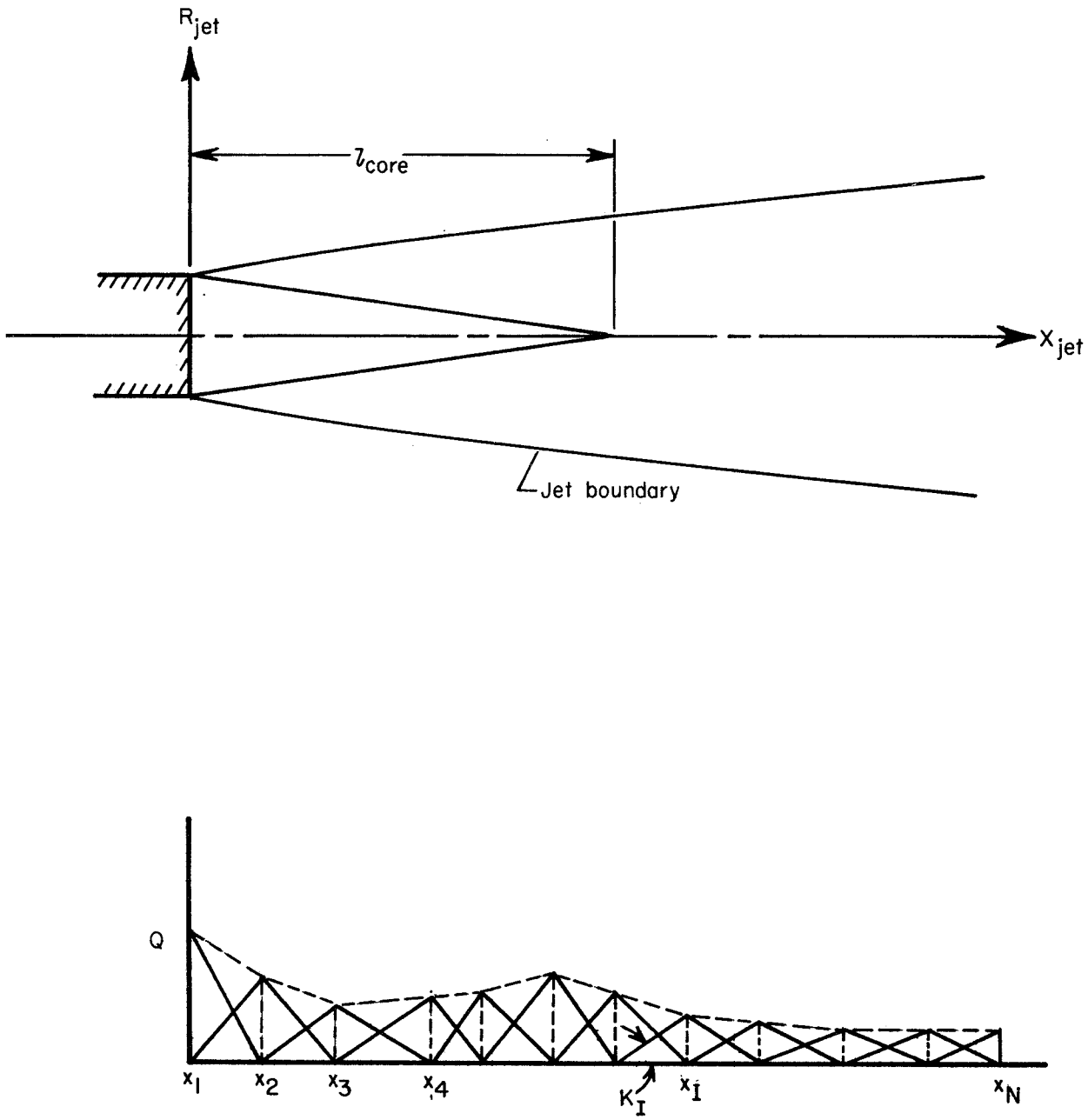

Figure 3.- Illustration of source-sink distribution used to represent effects of jet exhaust.

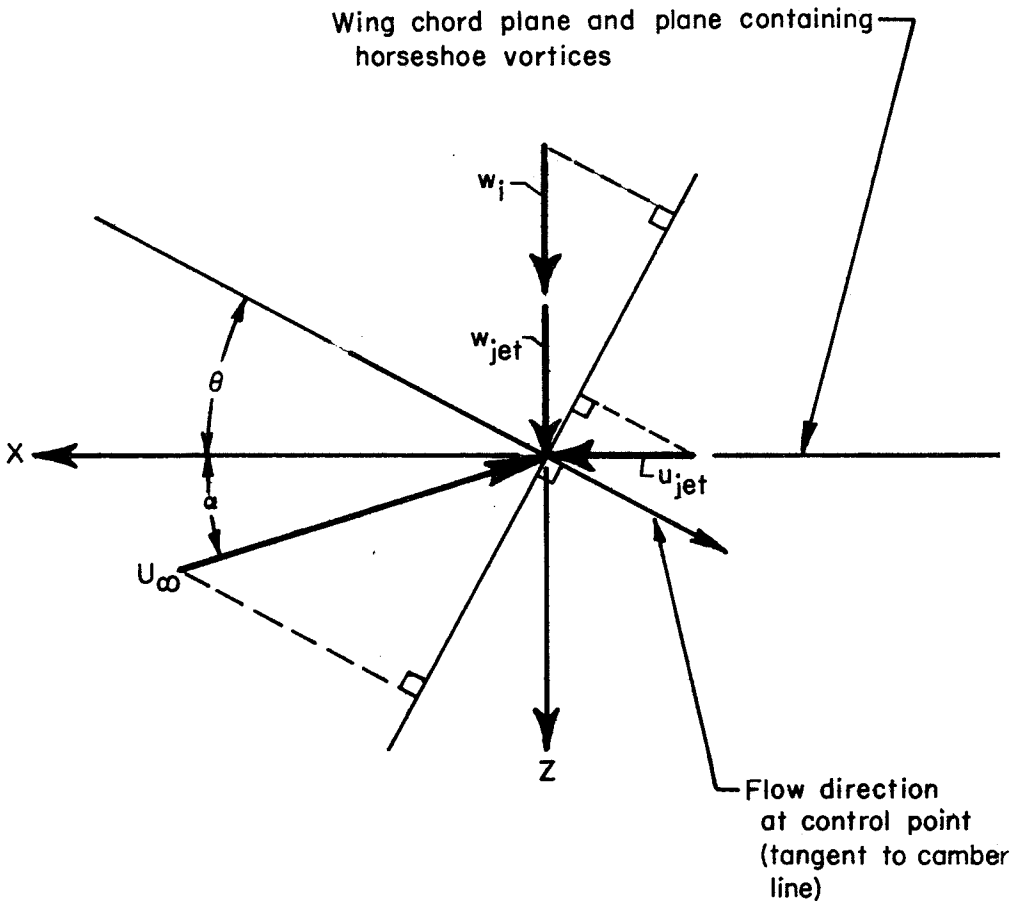

Boundary condition:

$$U_\infty \sin(\alpha + \theta) = (w_i + w_{jet}) \cos\theta + u_{jet} \sin\theta$$

Figure 4.- Sketch illustrating boundary conditions at each control point on a wing with camber.

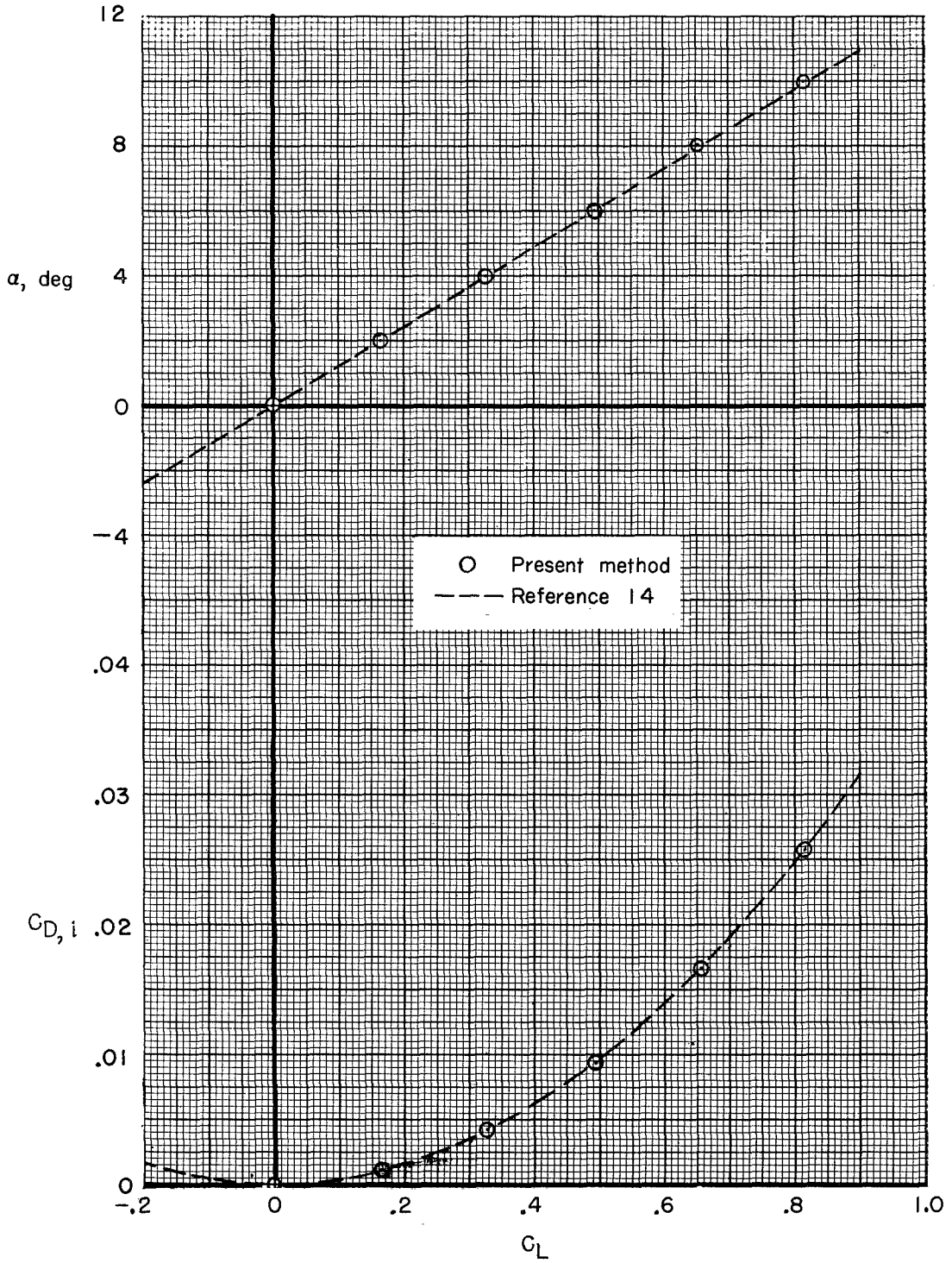

(a) Flat wing.

Figure 5.- Comparison of present method with that of reference 14 for an aspect-ratio-8, $\lambda = 1.0$ straight wing (jet off). (Near-field solution of ref. 14 for induced drag is shown.)

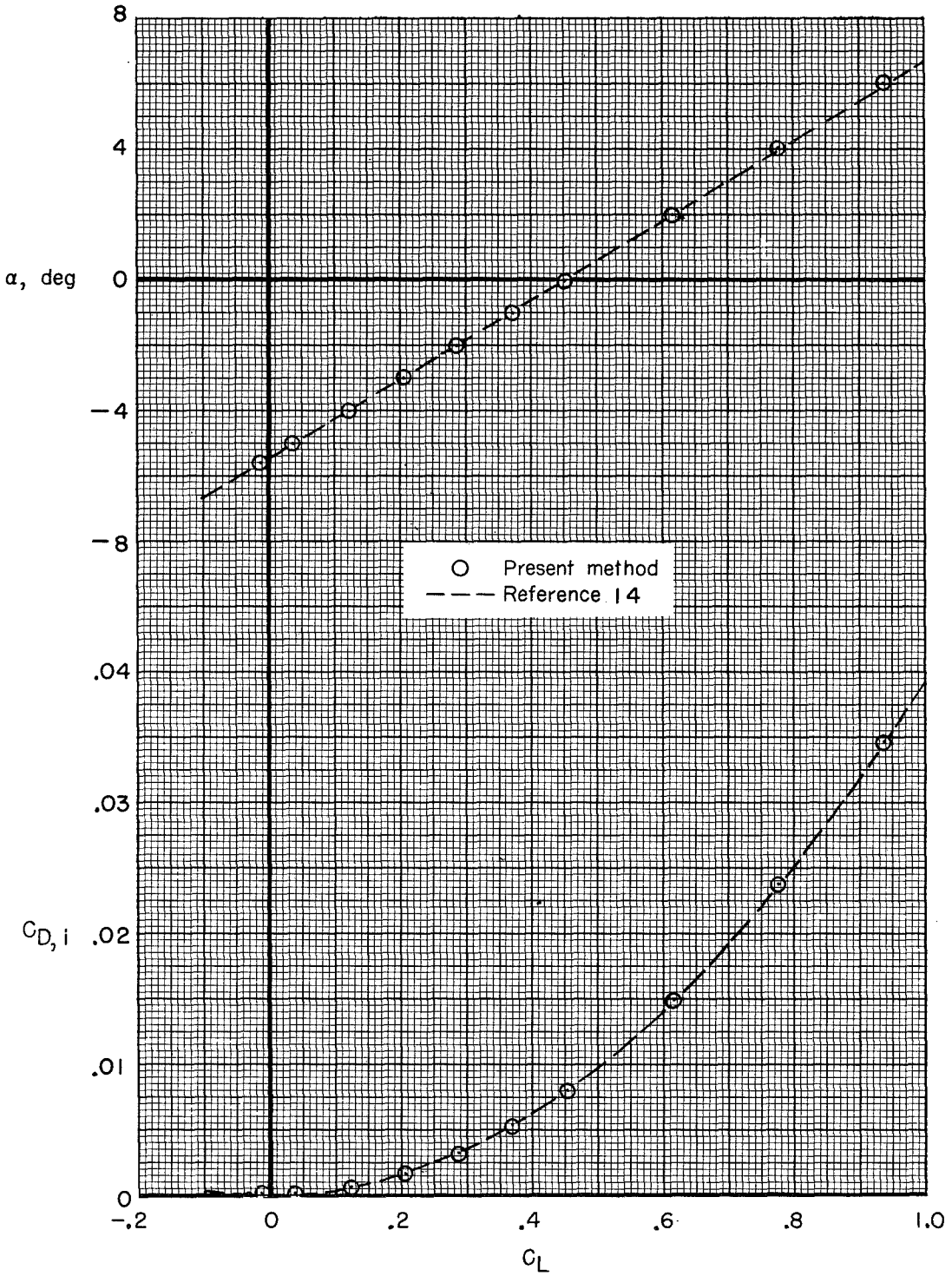

(b) Wing with Clark Y camber distribution.

Figure 5.- Continued.

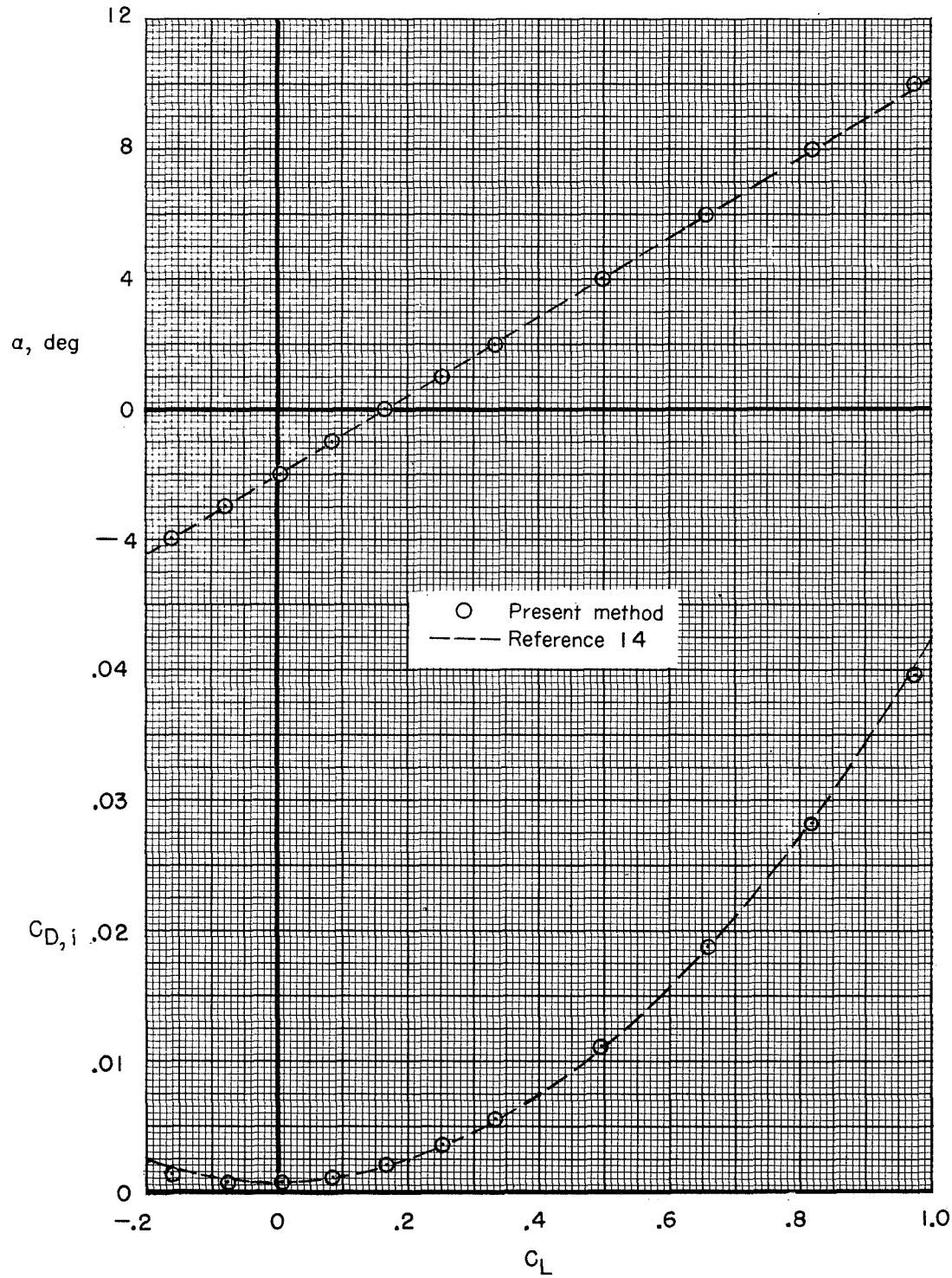

(c) Wing with twist distribution.

Figure 5.- Concluded.

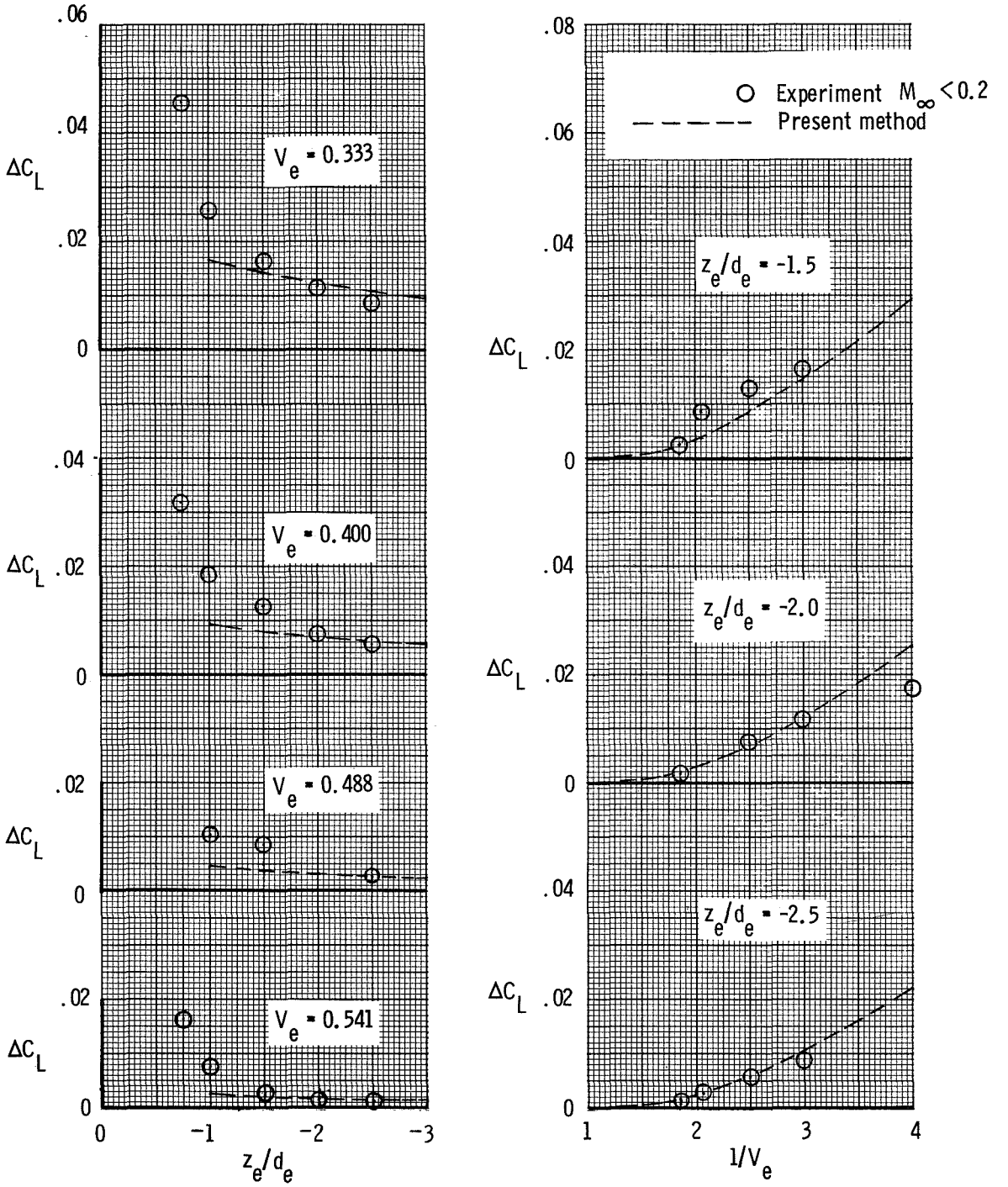

Figure 6.- Comparision of present method with experimental data of reference 17 for blowing one jet over an aspect-ratio-2, $\lambda = 1$ straight wing. $A_e/S_{ref} = 0.192$, $\left(x_e - x_{le}\right)/d_e = 1.0$, $\eta_e = 0.0$, $c_e/d_e = 6.250$, and $\alpha = 0^o$.

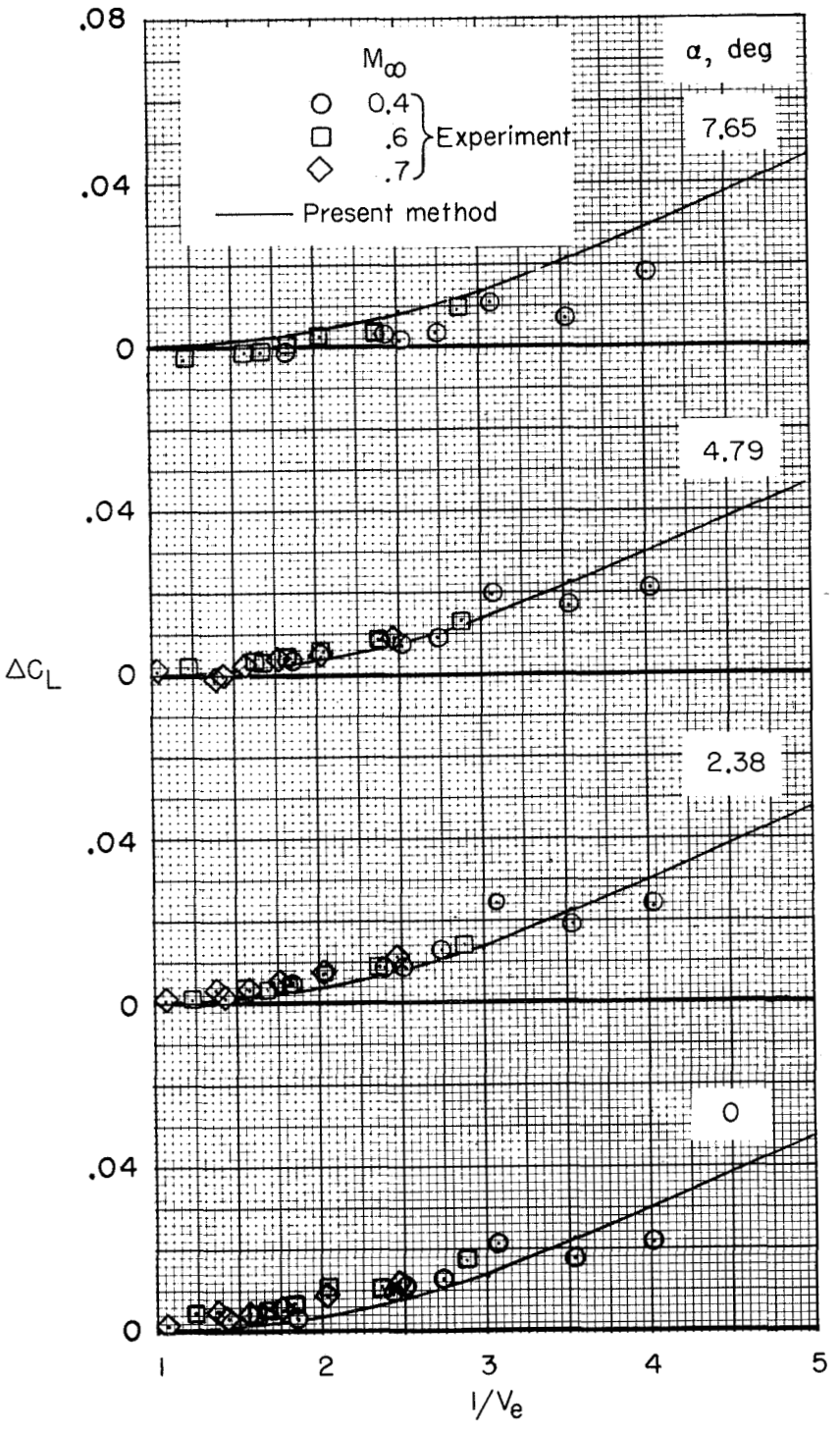

(a) Interference lift coefficient.

Figure 7.- Comparison of the present method with experimental data of reference 9 for two jets blowing over a wing with aspect ratio 3, $\lambda = 0.3$, and $\Lambda_{le} = 50^{o}$. $A_e/S_{ref} = 0.0078$, $\left(x_e - x_{le}\right)/d_e = 2.59$, $\eta_e = 0.46$, and $z_e/d_e = -1.5$.

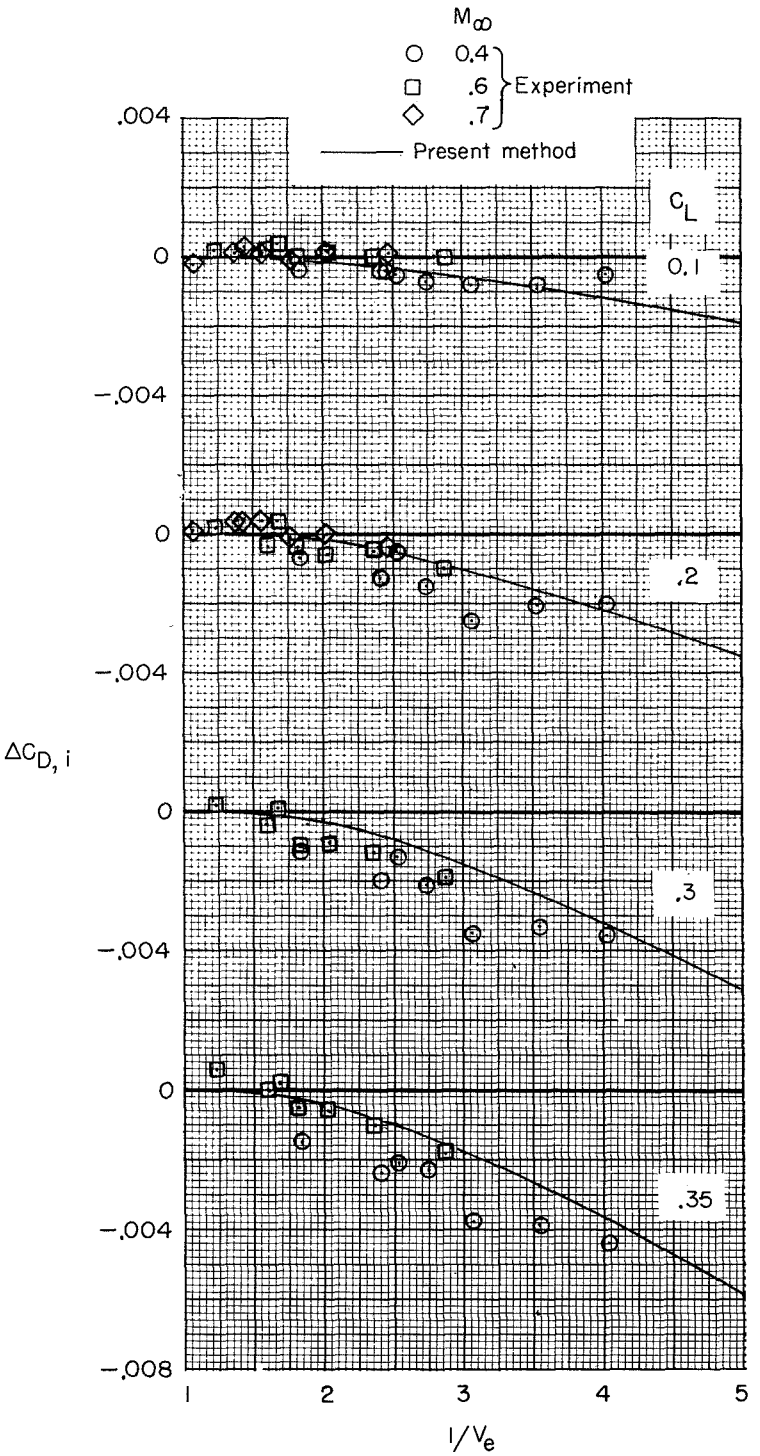

(b) Interference induced drag coefficient.

Figure 7.- Continued.

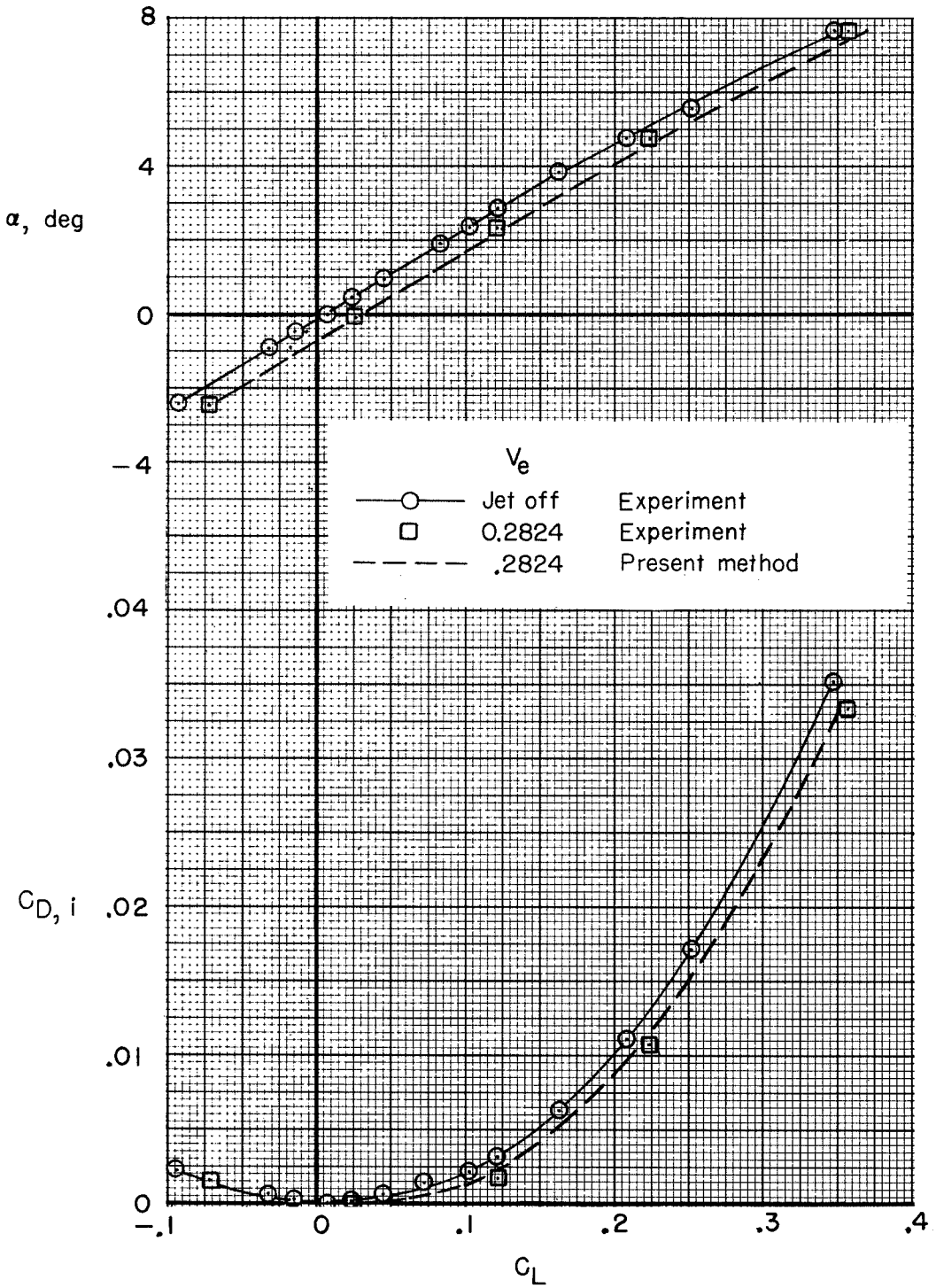

(c) Effect of jet blowing on lift and drag coefficient at $M_\infty = 0.40$.

Figure 7.- Concluded.

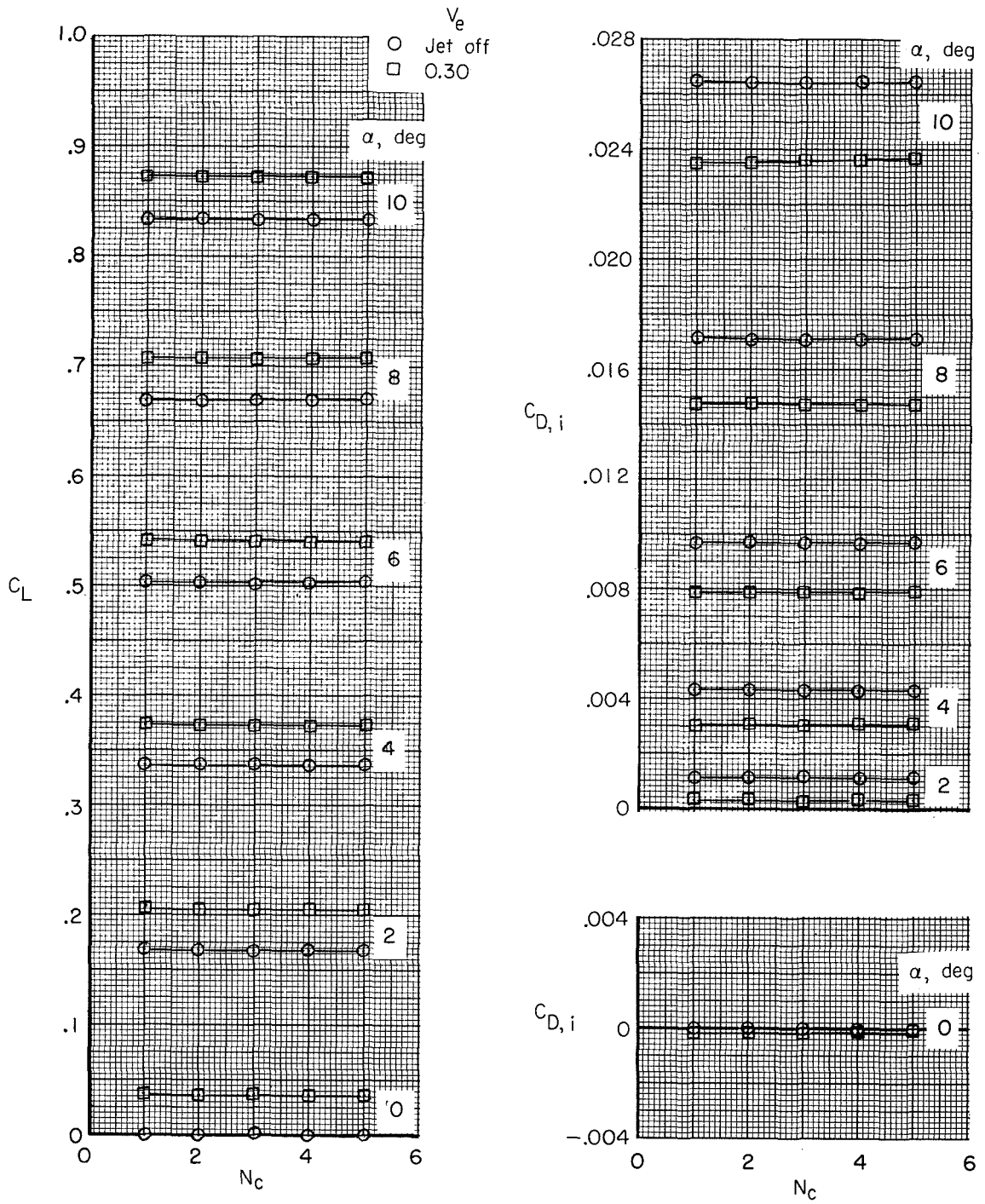

Figure 8.- Effect of number of chordwise elemental vortex-lattice panels when $N_S = 10$ on the calculated lift and induced drag of a wing with aspect ratio 8, $\lambda = 0.3$, and $\Lambda_{c/4} = 0^o$ and with two jets having $A_e/S_{ref} = 0.025$ located at $\left(x_e - x_{le}\right)/d_e = 0.0$, $\eta_e = 0.3$, $z_e/d_e = -1.5$, and $c_e/d_e = 2.408$.

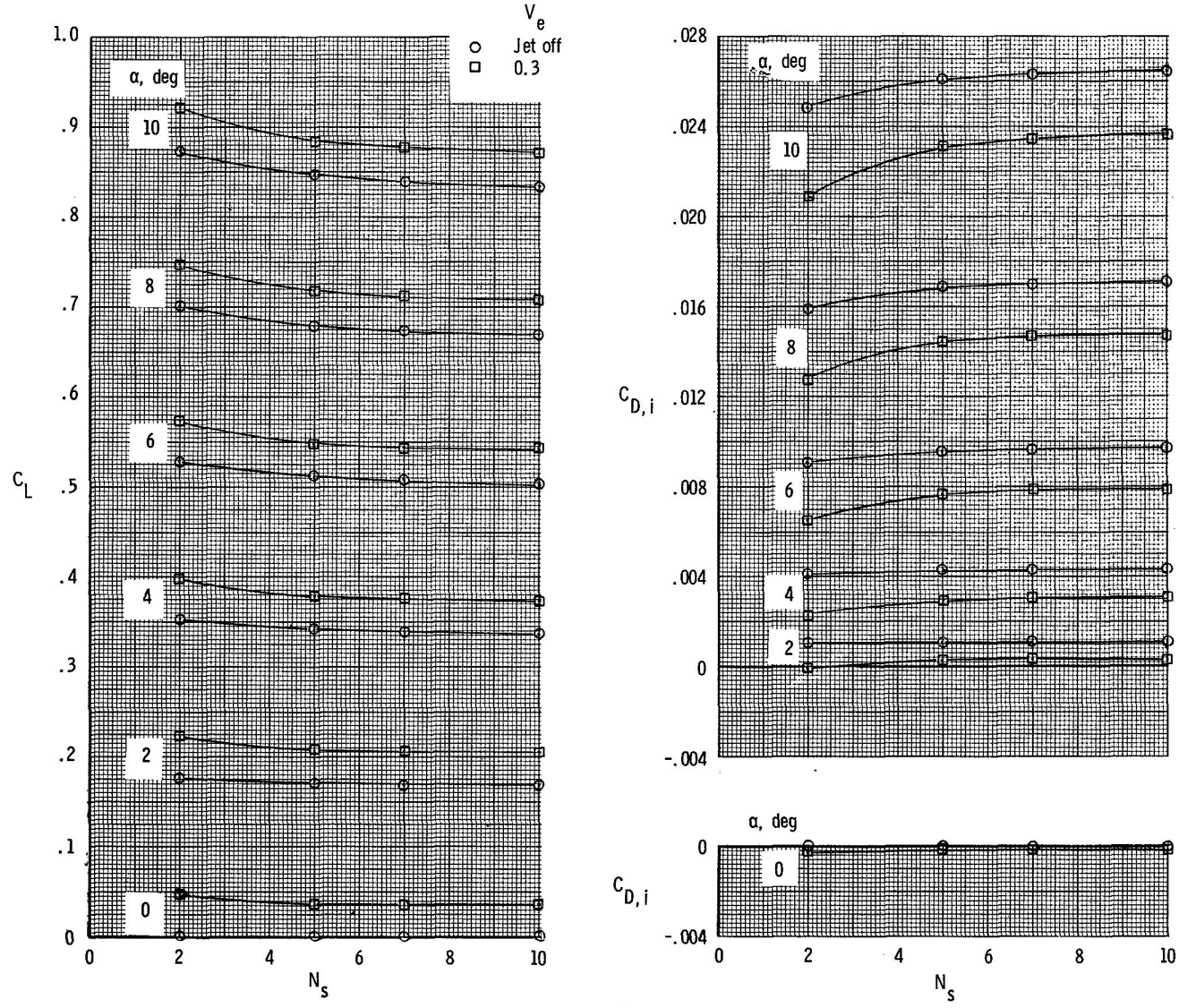

Figure 9.- Effect of the number of spanwise elemental vortex-lattice panels when $N_c = 5$ on the calculated lift and induced drag of a wing with aspect ratio 8, $\lambda = 0.3$, and $\Lambda_{c/4} = 0^o$ and with two jets having $A_e/S_{ref} = 0.025$ located at $\left(x_e - x_{le}\right)/d_e = 0.0$, $\eta_e = 0.3$, $z_e/d_e = -1.5$, and $c_e/d_e = 2.408$.

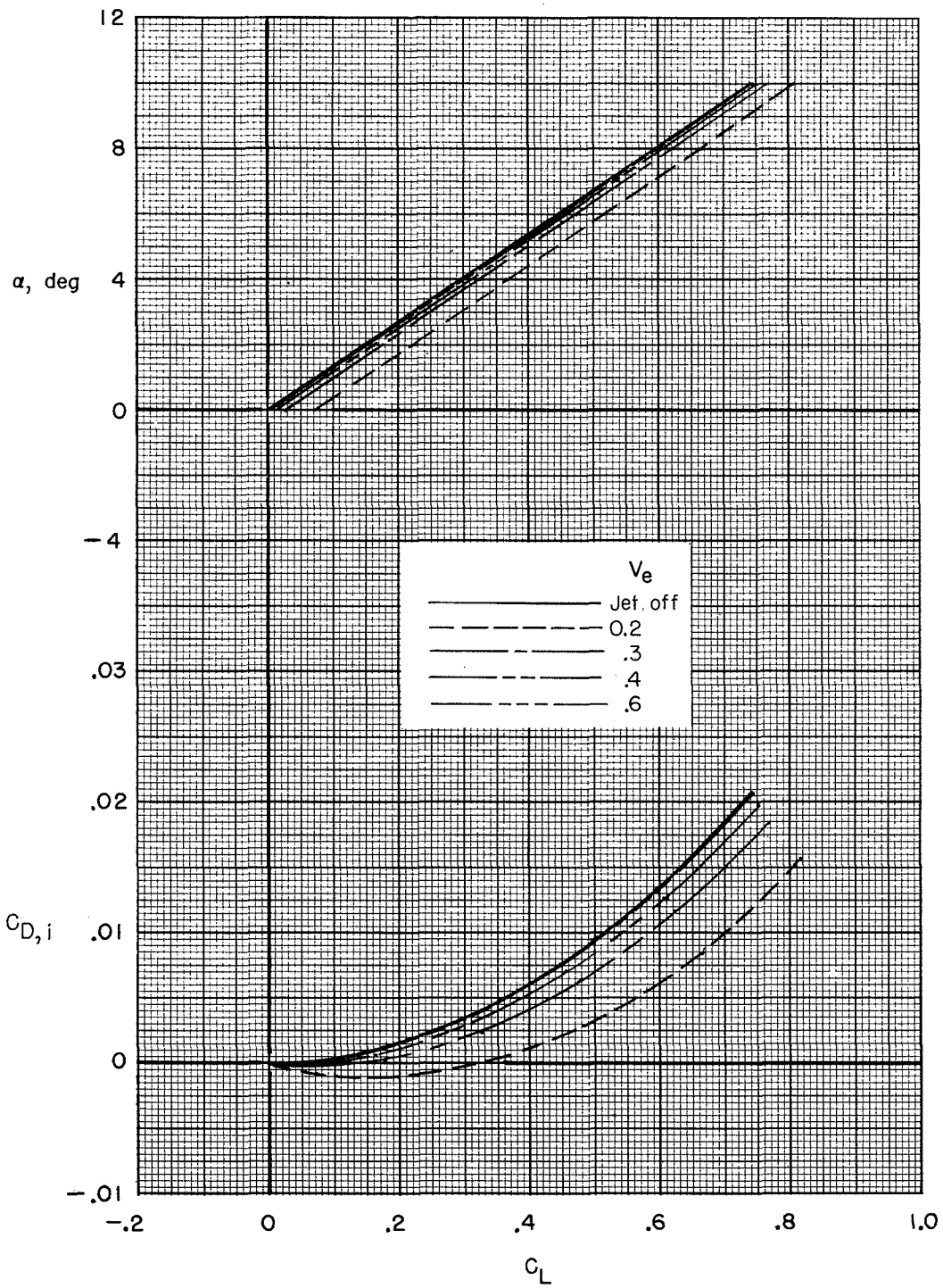

(a) Effect on C_L and $C_{D,i}$.

Figure 10.- Calculated effect of effective velocity ratio of two jets on aerodynamic characteristics of a wing with aspect ratio 8, $\lambda = 0.3$, and $\Lambda_{c/4} = 30^{\circ}$, $A_e/S_{ref} = 0.0125$, $\left(x_e - x_{le}\right)/d_e = 0.0$, $\eta_e = 0.25$, $z_e/d_e = -1.401$, and $c_e/d_e = 3.557$.

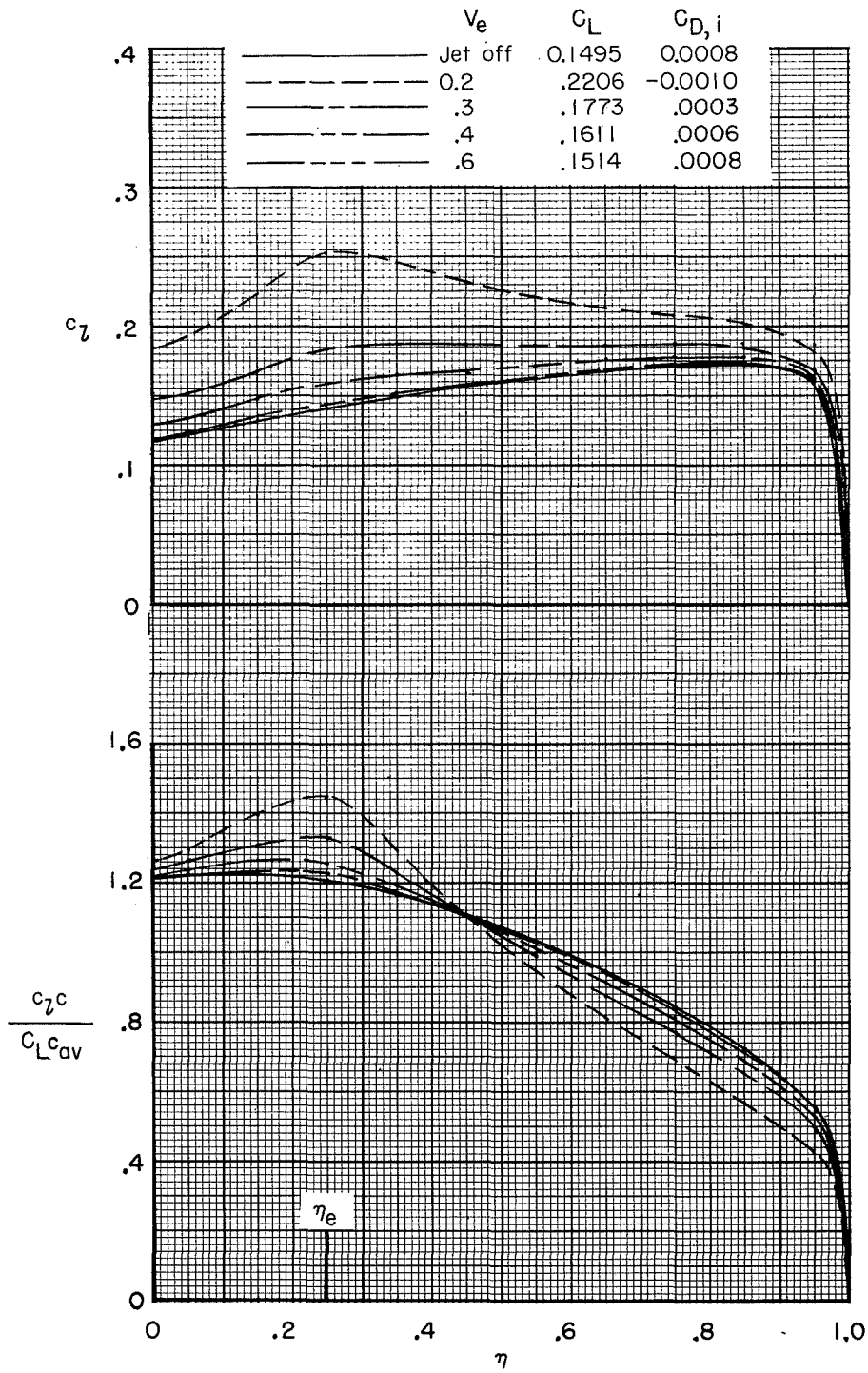

(b) Effect on span load distribution and section lift coefficient at $\alpha = 2^{\circ}$.

Figure 10.- Continued.

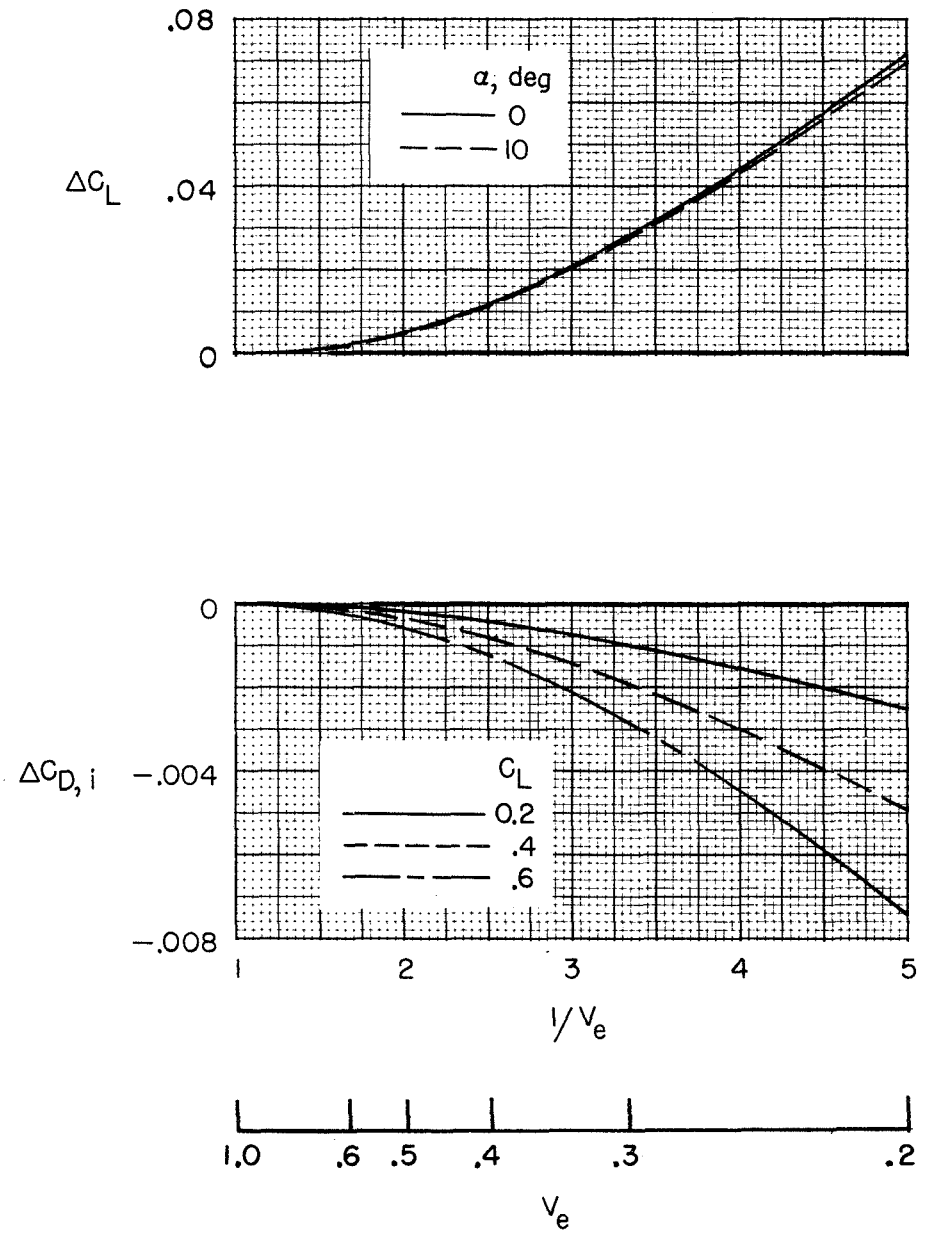

(c) Effect on ΔC_L and $\Delta C_{D,i}$.

Figure 10.- Concluded.

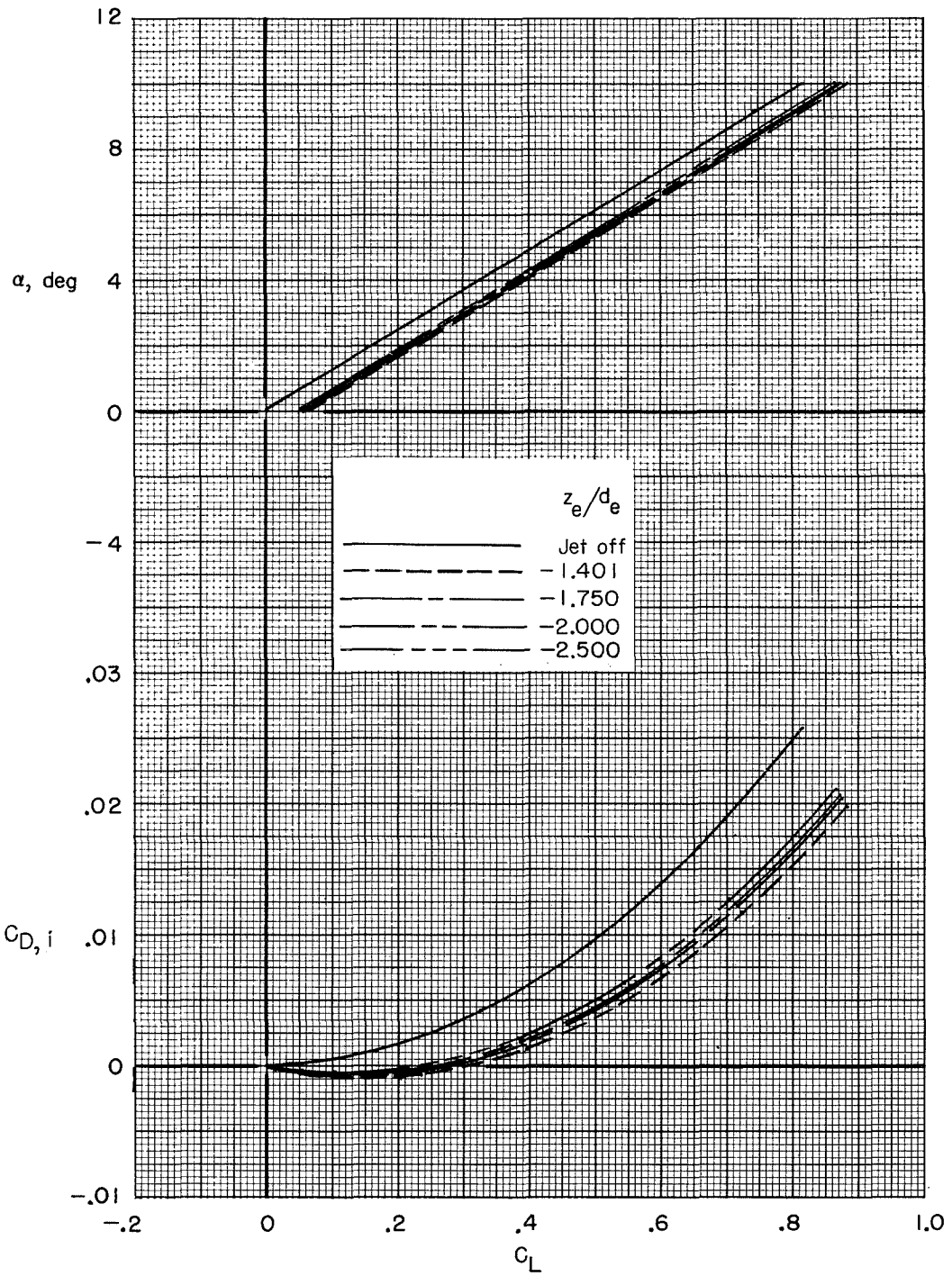

(a) Effect on C_L and $C_{D,i}$.

Figure 11.- Calculated effect of vertical location of two jets on aerodynamic characteristics of an aspect-ratio-8, $\lambda = 1.0$ straight wing. $A_e/S_{ref} = 0.0125$, $V_e = 0.20$, $\eta_e = 0.25$, $\left(x_e - x_{le}\right)/d_e = 0.0$, and $c_e/d_e = 2.803$.

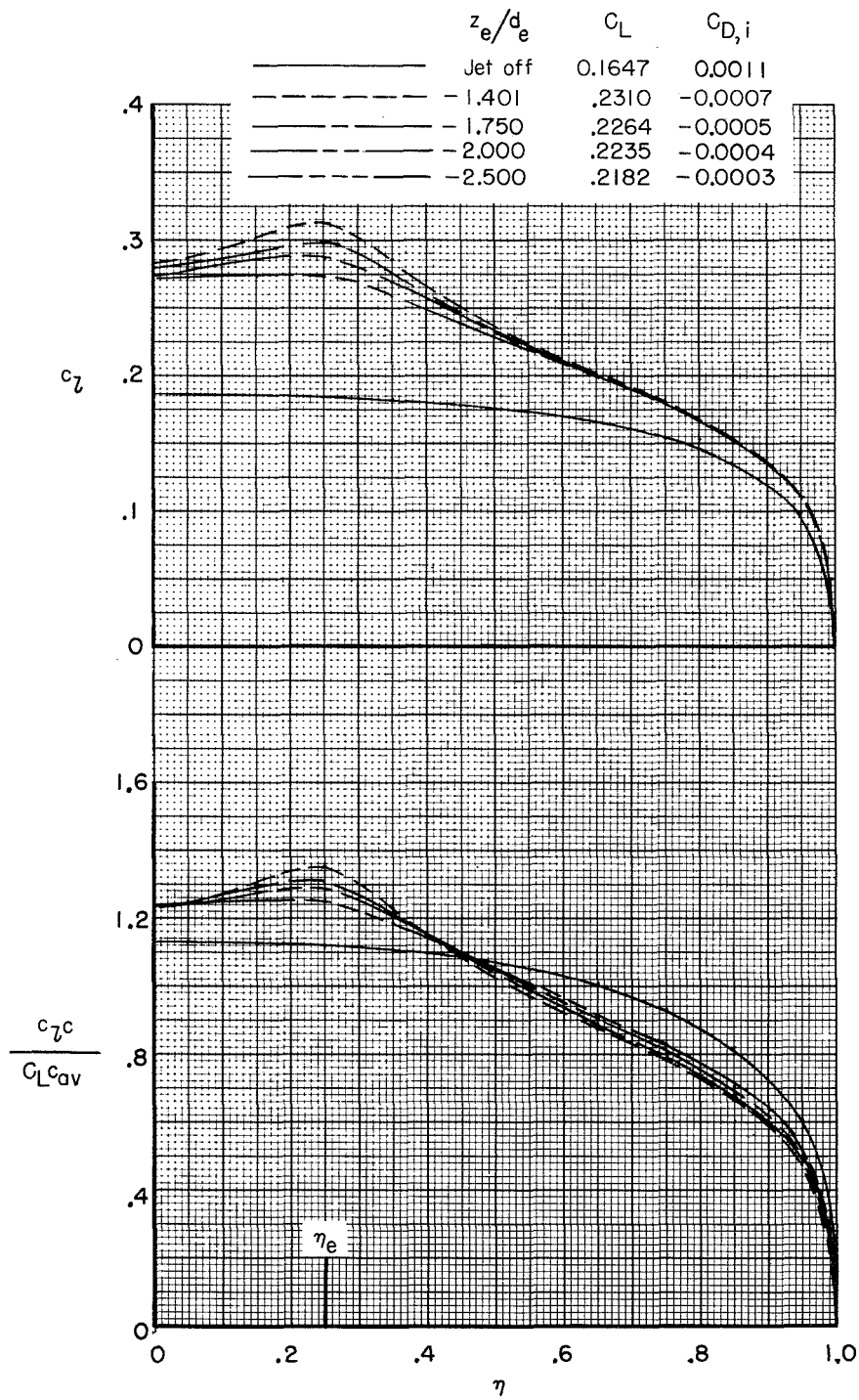

(b) Effect on span load distribution and section lift coefficient at $\alpha = 2^{\circ}$.

Figure 11.- Continued.

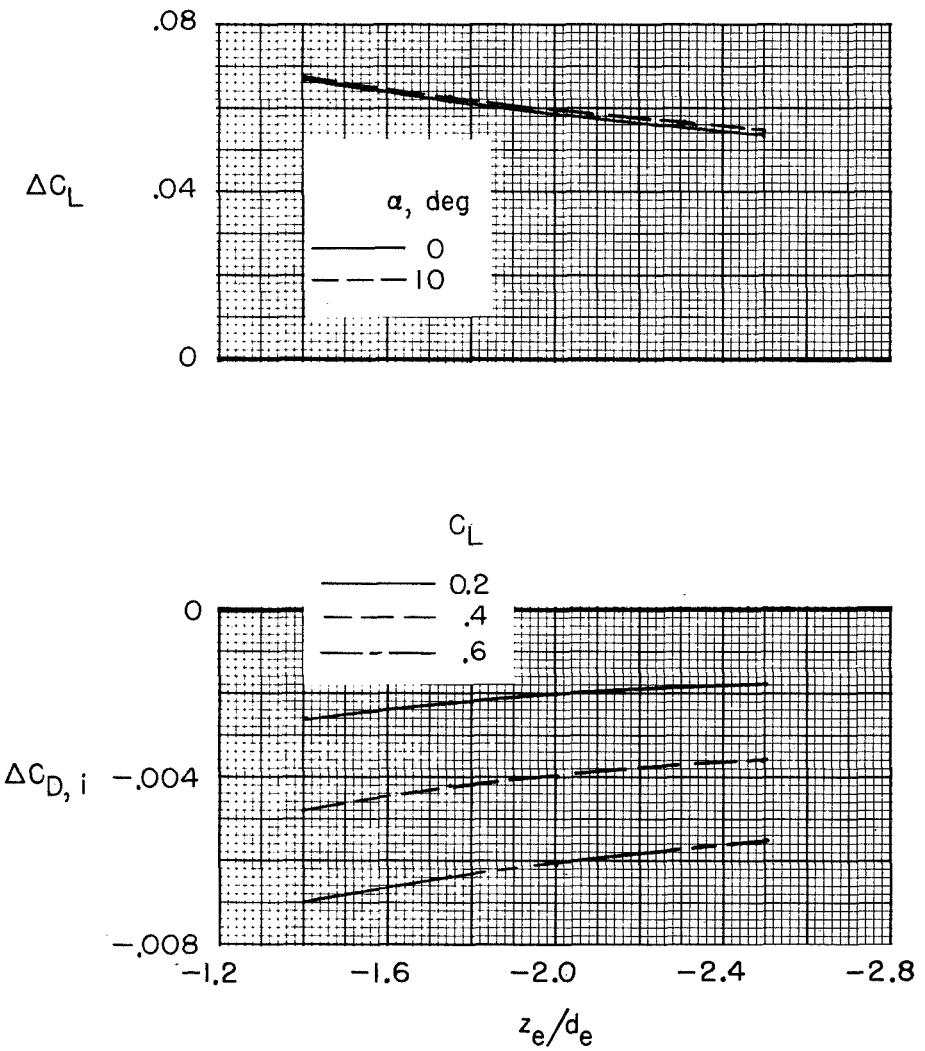

(c) Effect on ΔC_L and $\Delta C_{D,i}$.

Figure 11.- Concluded.

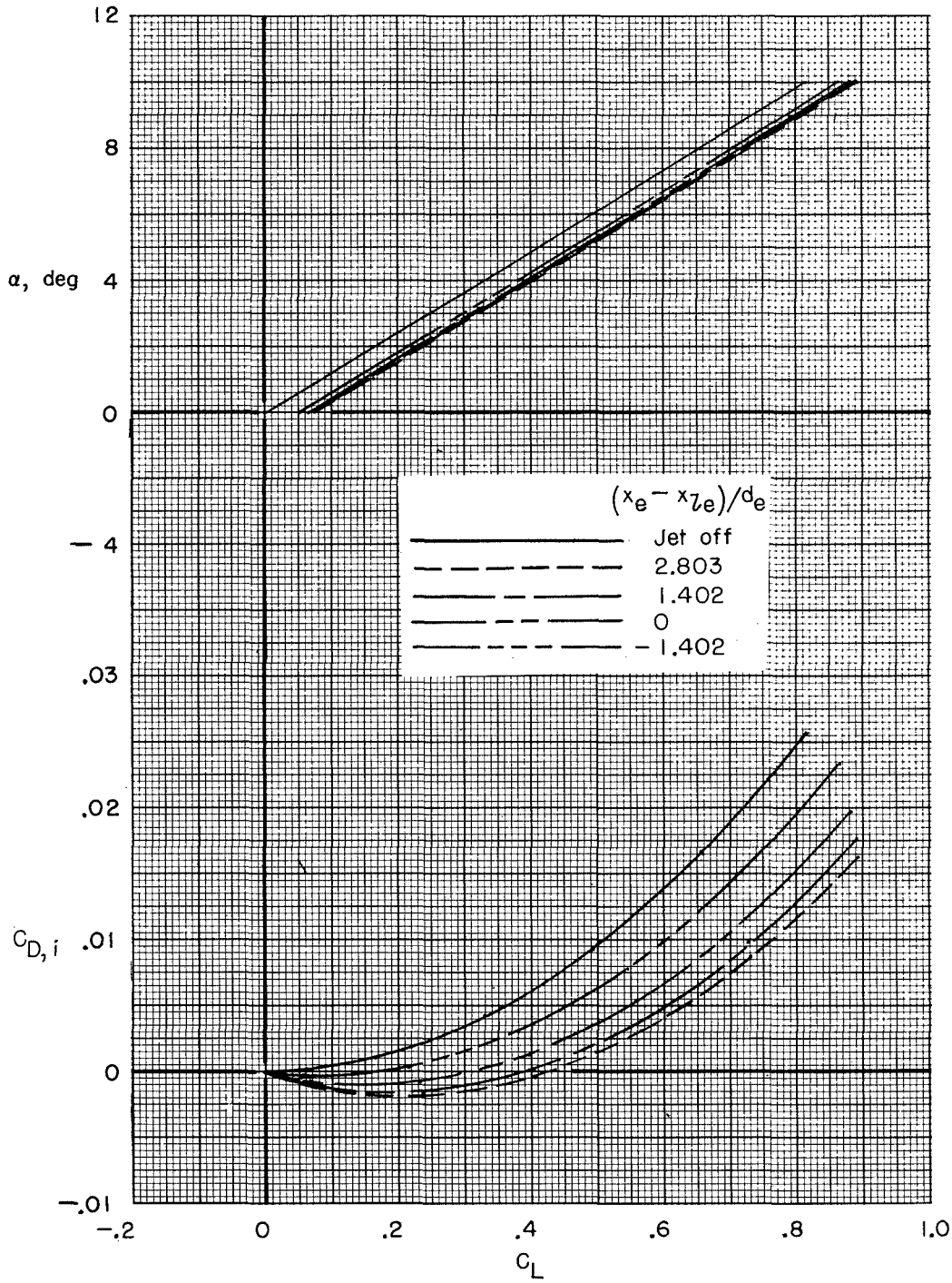

(a) Effect on C_L and $C_{D,i}$.

Figure 12.- Calculated effect of longitudinal location of two jets on aerodynamic characteristics of an aspect-ratio-8, $\lambda = 1.0$ straight wing. $A_e/S_{ref} = 0.0125$, $V_e = 0.20$, $\eta_e = 0.25$, $z_e/d_e = -1.401$, and $c_e/d_e = 2.803$.

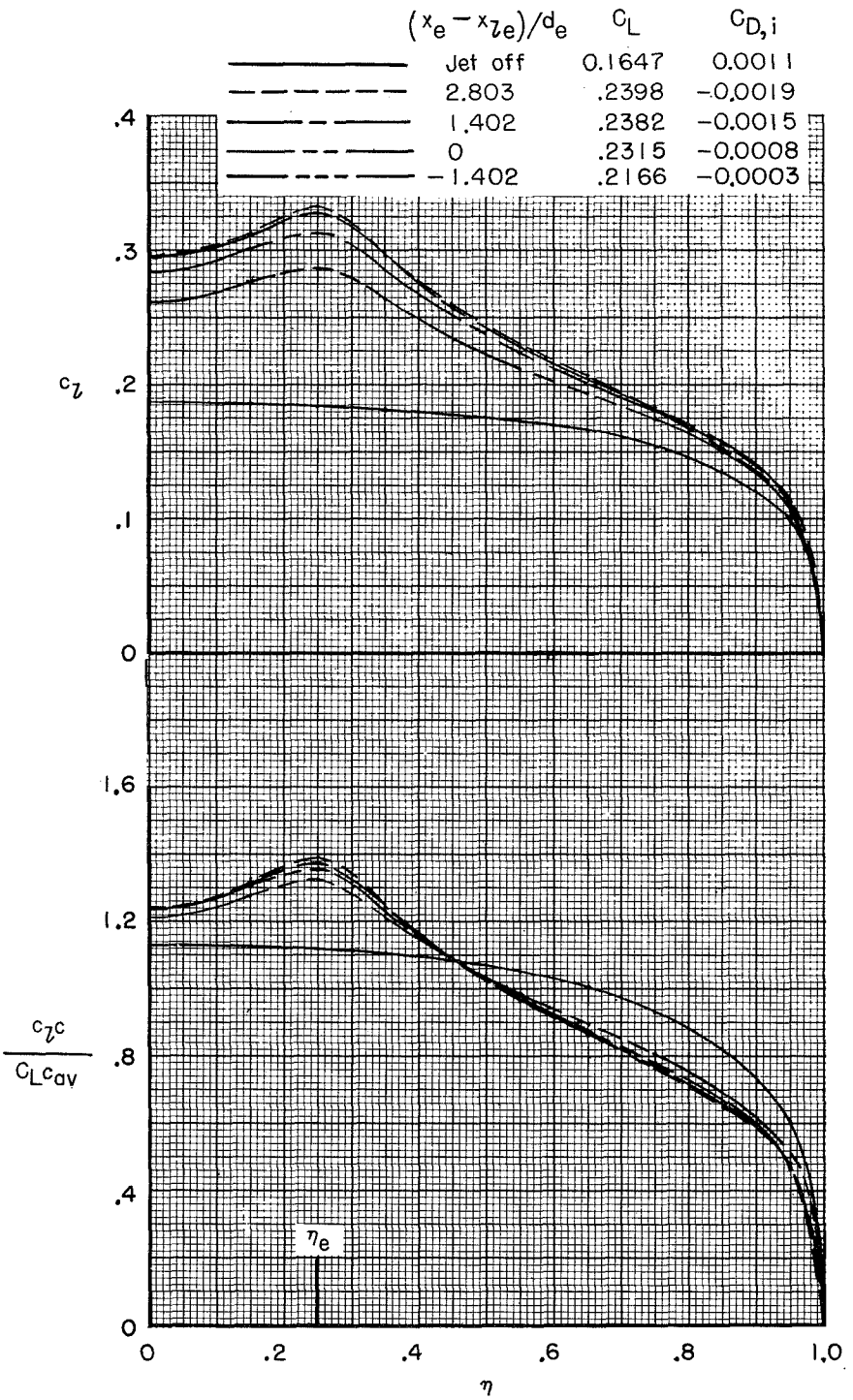

(b) Effect on span load distribution and section lift coefficient at $\alpha = 2^{\circ}$.

Figure 12.- Continued.

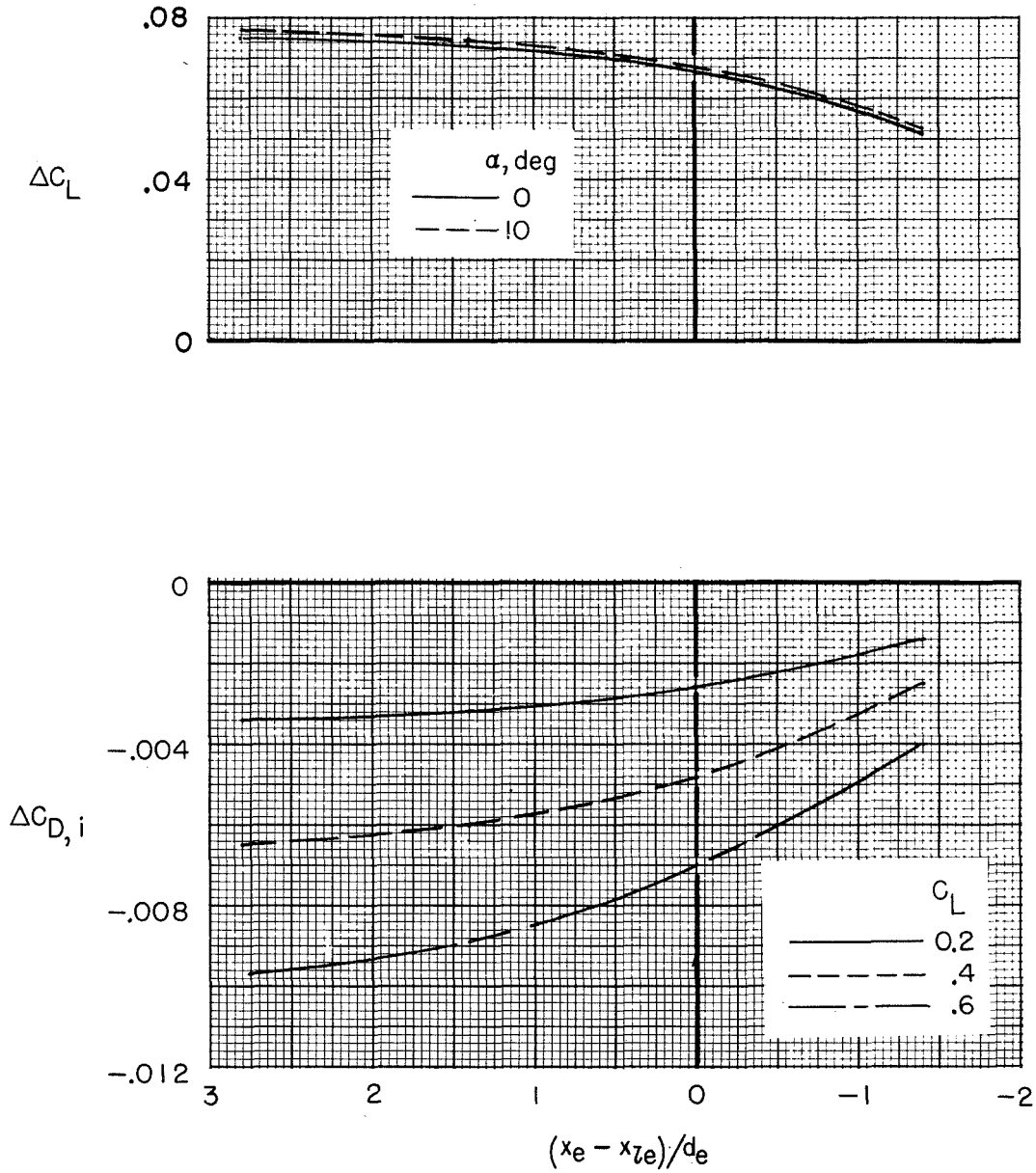

(c) Effect on ΔC_L and $\Delta C_{D,i}$.

Figure 12.- Concluded.

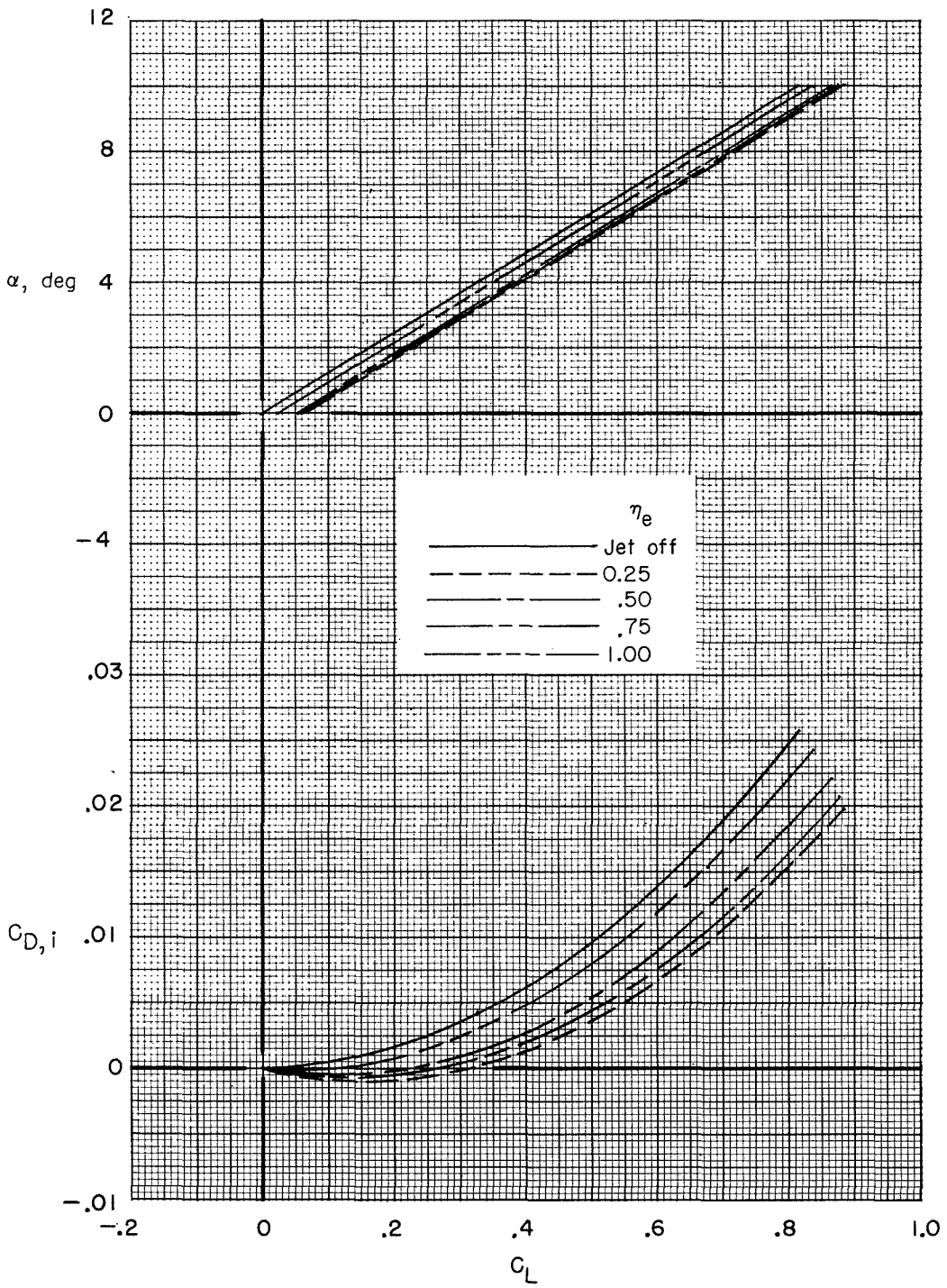

(a) Effect on C_L and $C_{D,i}$.

Figure 13.- Calculated effect of lateral location of two jets on aerodynamic characteristics of an aspect-ratio-8, $\lambda = 1.0$ straight wing. $A_e/S_{ref} = 0.0125$, $V_e = 0.20$, $\left(x_e - x_{le}\right)/d_e = 0.0$, $z_e/d_e = -1.401$, and $c_e/d_e = 2.803$.

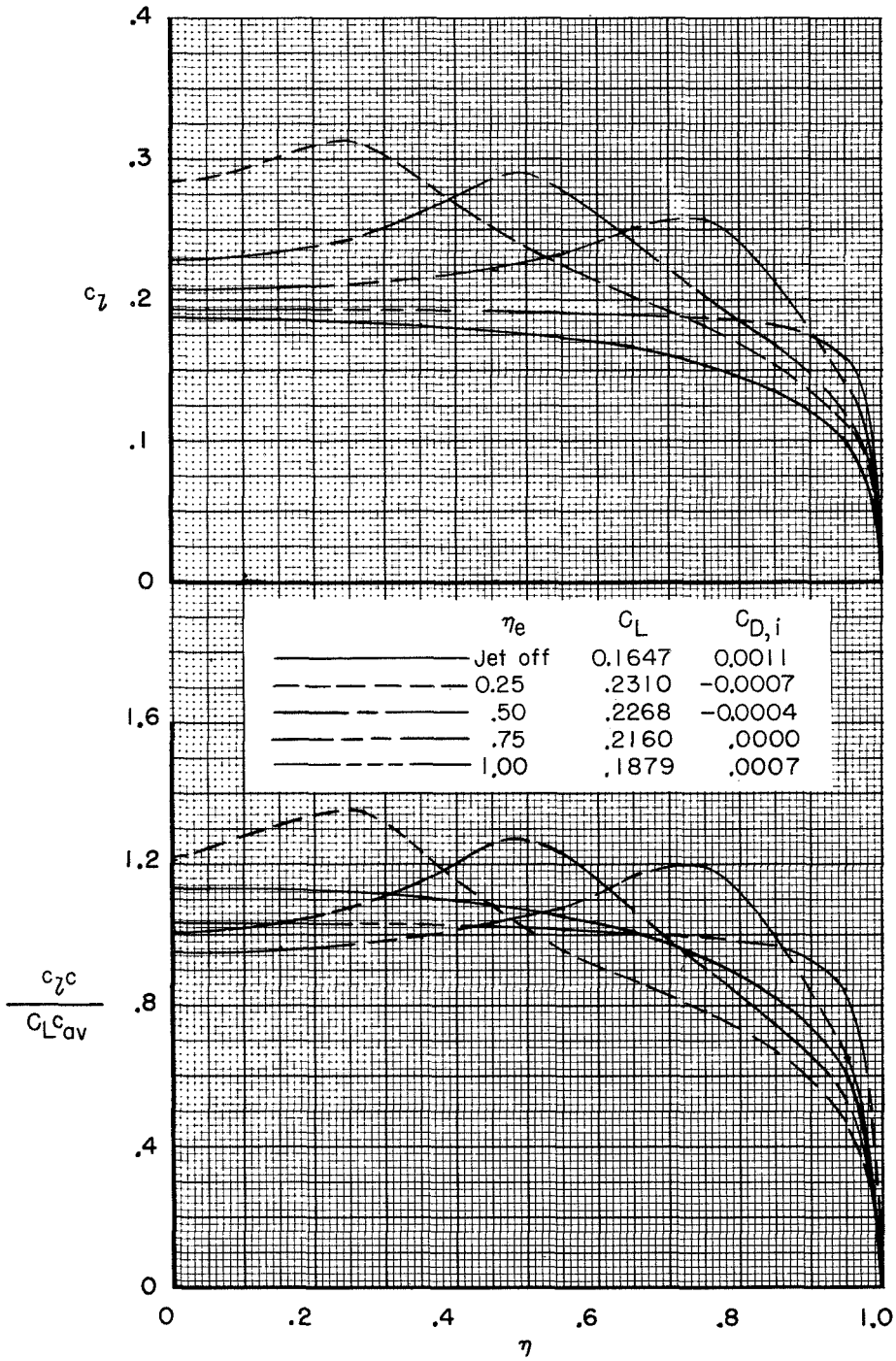

(b) Effect on span load distribution and section lift coefficient at $\alpha = 2^{\circ}$.

Figure 13.- Continued.

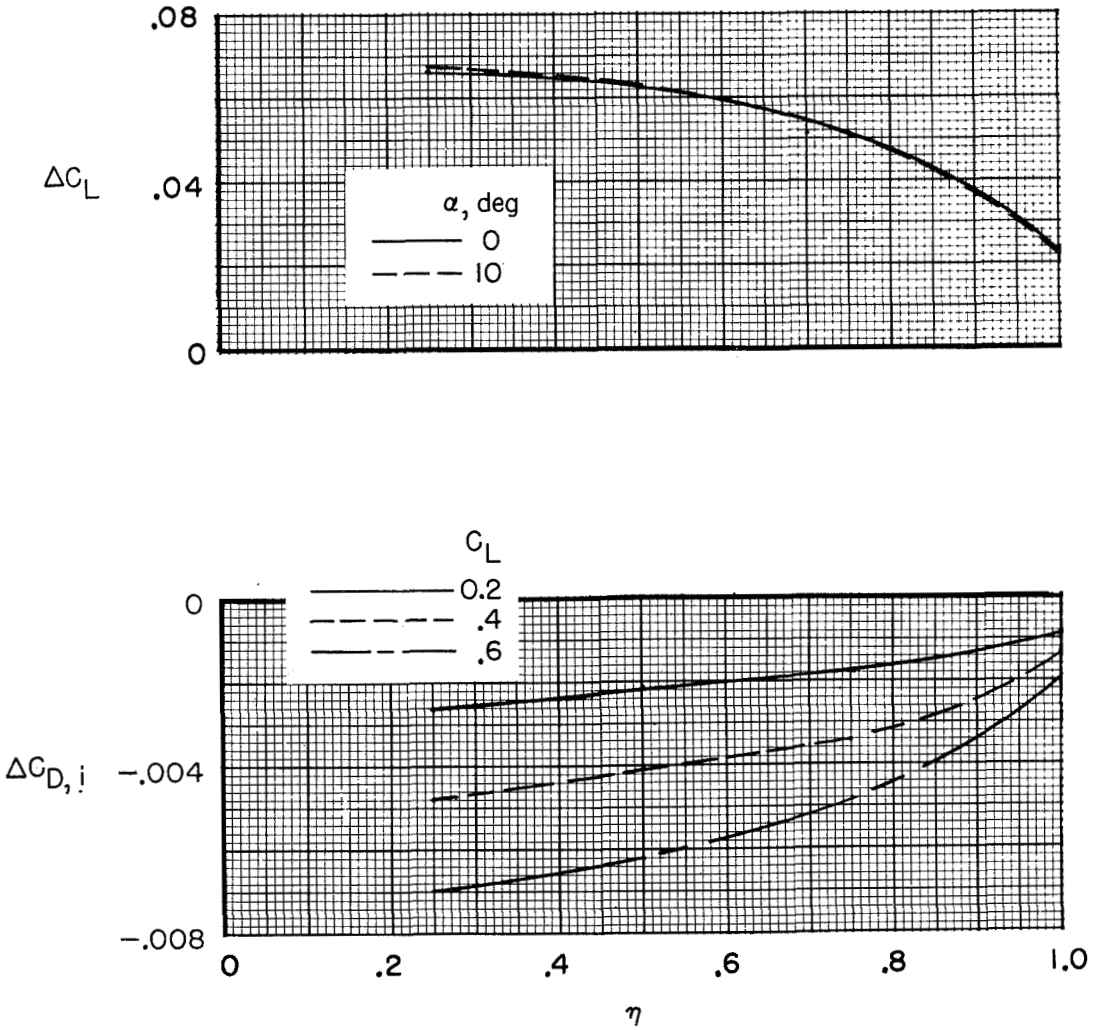

(c) Effect on ΔC_L and $\Delta C_{D,i}$.

Figure 13.- Concluded.

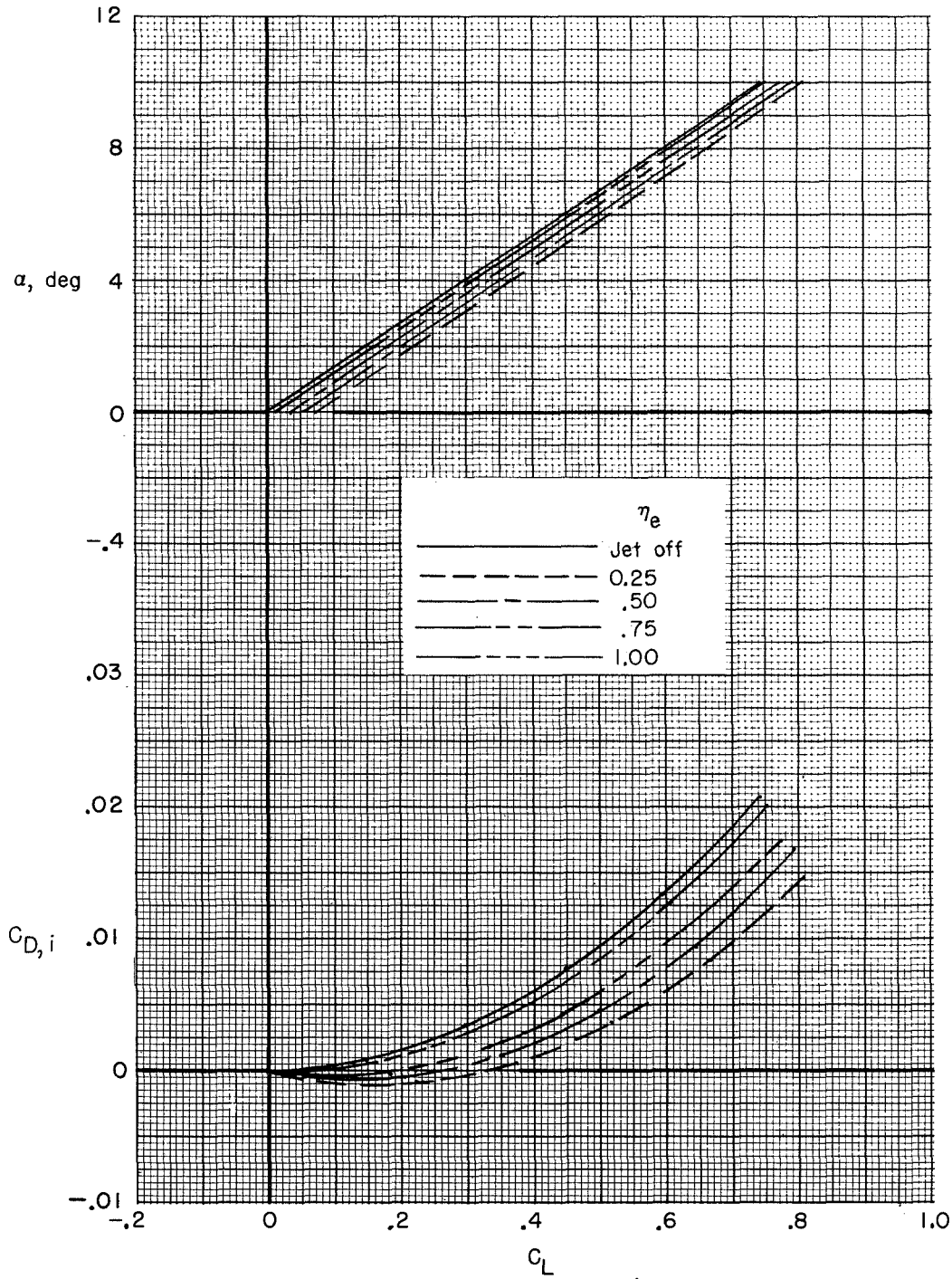

(a) Effect on C_L and $C_{D,i}$.

Figure 14.- Calculated effect of lateral location of two jets on aerodynamic characteristics of a wing with aspect ratio 8, $\lambda = 0.3$, and $\Lambda_{c/4} = 30^o$. $A_e/S_{ref} = 0.0125$, $V_e = 0.20$, $\left(x_e - x_{le}\right)/d_e = 0.0$, and $z_e/d_e = -1.401$.

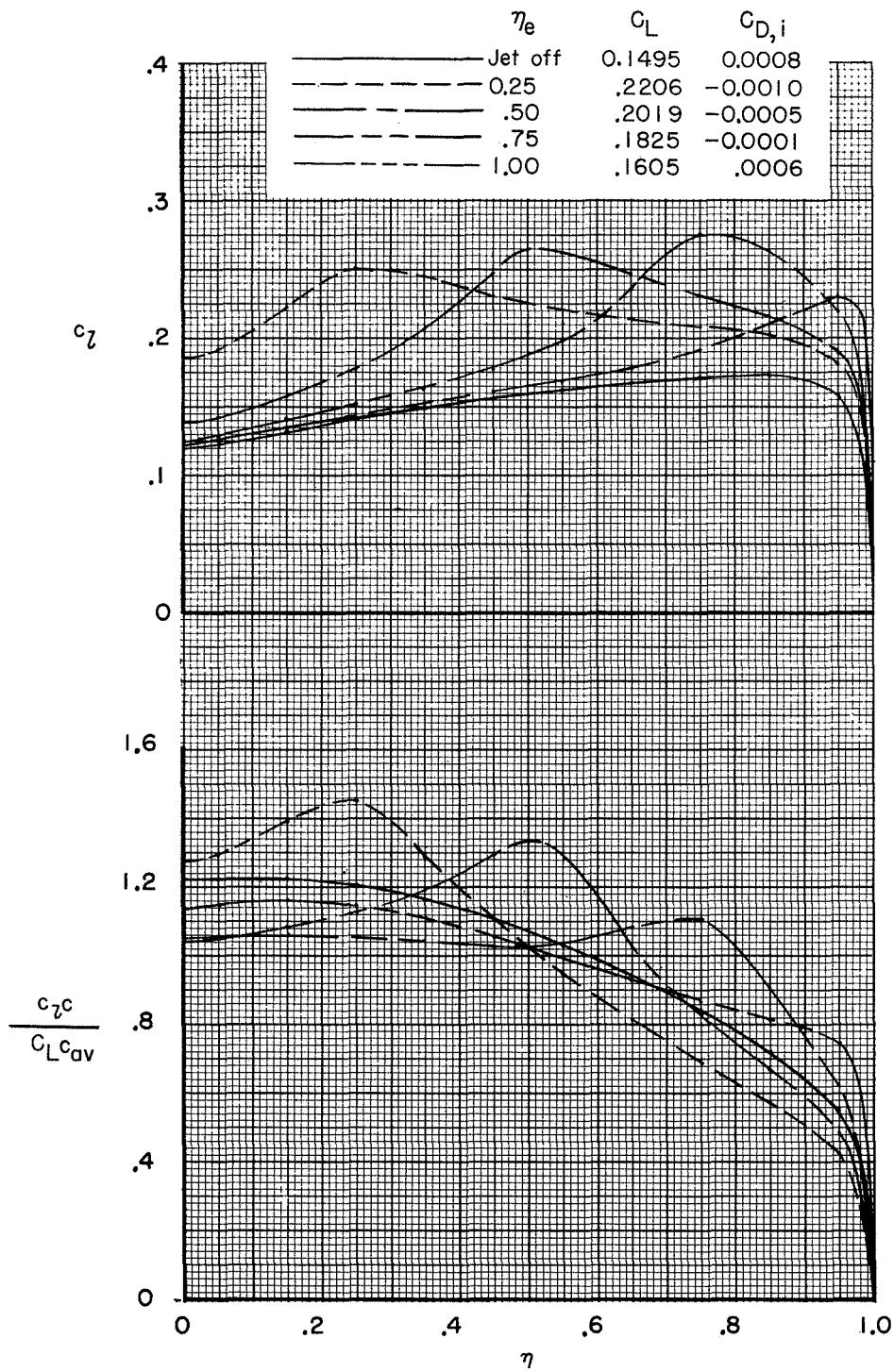

(b) Effect on span load distribution and section lift coefficient at $\alpha = 2^{\circ}$.

Figure 14.- Continued.

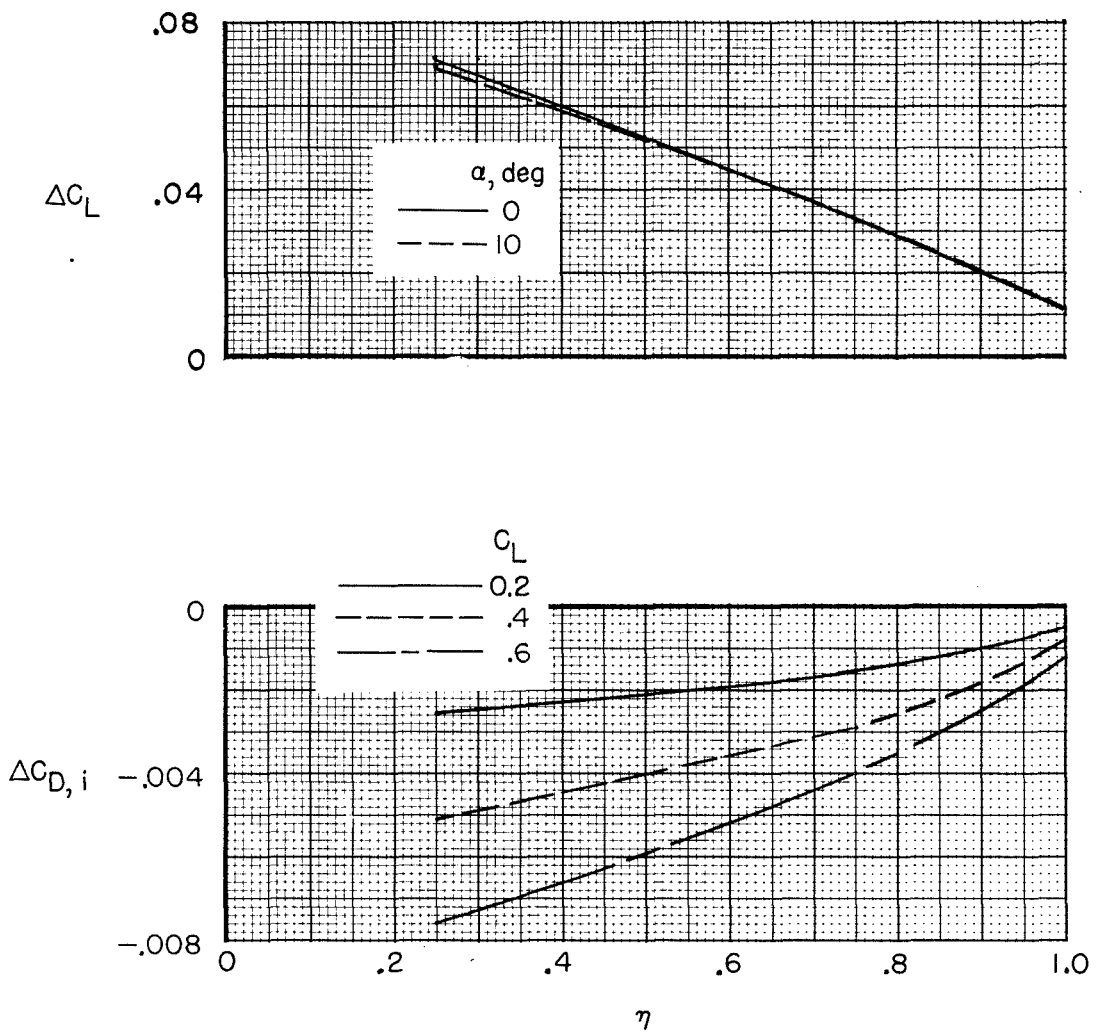

(c) Effect on ΔC_L and $\Delta C_{D,i}$.

Figure 14.- Concluded.

NATIONAL AERONAUTICS AND SPACE ADMINISTRATION
WASHINGTON, D.C. 20546

OFFICIAL BUSINESS
PENALTY FOR PRIVATE USE $300

SPECIAL FOURTH-CLASS RATE BOOK

POSTAGE AND FEES PAID
NATIONAL AERONAUTICS AND SPACE ADMINISTRATION
451

U.S.MAIL

POSTMASTER: If Undeliverable (Section 158 Postal Manual) Do Not Return

"The aeronautical and space activities of the United States shall be conducted so as to contribute . . . to the expansion of human knowledge of phenomena in the atmosphere and space. The Administration shall provide for the widest practicable and appropriate dissemination of information concerning its activities and the results thereof."

—NATIONAL AERONAUTICS AND SPACE ACT OF 1958

NASA SCIENTIFIC AND TECHNICAL PUBLICATIONS

TECHNICAL REPORTS: Scientific and technical information considered important, complete, and a lasting contribution to existing knowledge.

TECHNICAL NOTES: Information less broad in scope but nevertheless of importance as a contribution to existing knowledge.

TECHNICAL MEMORANDUMS: Information receiving limited distribution because of preliminary data, security classification, or other reasons. Also includes conference proceedings with either limited or unlimited distribution.

CONTRACTOR REPORTS: Scientific and technical information generated under a NASA contract or grant and considered an important contribution to existing knowledge.

TECHNICAL TRANSLATIONS: Information published in a foreign language considered to merit NASA distribution in English.

SPECIAL PUBLICATIONS: Information derived from or of value to NASA activities. Publications include final reports of major projects, monographs, data compilations, handbooks, sourcebooks, and special bibliographies.

TECHNOLOGY UTILIZATION PUBLICATIONS: Information on technology used by NASA that may be of particular interest in commercial and other non-aerospace applications. Publications include Tech Briefs, Technology Utilization Reports and Technology Surveys.

Details on the availability of these publications may be obtained from:

SCIENTIFIC AND TECHNICAL INFORMATION OFFICE

NATIONAL AERONAUTICS AND SPACE ADMINISTRATION

Washington, D.C. 20546